MACHINE LEARNING BASED RECEIVER DESIGN FOR RADAR COMMUNICATIONS

A Thesis

by

CHANDRA SHEKHARA KAUSHIK VALMEEKAM

Submitted to the Office of Graduate and Professional Studies of
Texas A&M University
in partial fulfillment of the requirements for the degree of

MASTER OF SCIENCE

Chair of Committee,	Krishna Narayanan
Committee Members,	Jean-Francois Chamberland
	Sebastian Hoyos
	Theodora Chaspari
Head of Department,	Miroslav M. Begovic

August 2020

Major Subject: Electrical Engineering

ABSTRACT

With increasing congestion of Radio Frequency (RF) spectrum, enabling radar and communication systems to coexist is becoming an important area of research for efficient spectrum utilization. Designing radar systems that can function amidst communication interference is a major step in this direction. The non optimality of matched filtering based receivers under communication interference provides the need to look for alternative approaches in radar receiver design. In this thesis we propose a machine learning based radar receiver design to tackle the problem of communication interference. Three different neural network architectures were designed and evaluated. The matched filtering based Constant False Alarm Rate (CFAR) detector was considered as a baseline for the evaluations. The performance of these detectors was evaluated on signal datasets generated from two sets of parameters each with different configurations of Signal to Noise Ratio (SNR) and interference power. The results obtained from the simulations depict that most of the evaluated neural network architectures significantly outperform the baseline CFAR detector in most configurations of SNR and interference power. This shows that the designed neural network architectures are able to learn some form of filtering better than the matched filter.

ACKNOWLEDGMENTS

Firstly, I would like to thank my parents for supporting me and bearing with all the inconsistencies I had in various aspects of my life. Secondly, I would like to sincerely thank my thesis advisor Prof. Krishna Narayanan who guided and stood as a stronghold during the preparation and presentation of this thesis. I would also like to thank the Texas A&M University and the department of Electrical and Computer Engineering for providing me with the right environment to learn and grow in my area of research. Lastly, I would like to express my deepest gratitude to my friends and family for providing me the moral support and encouragement. Special thanks to my younger brother for helping me throughout my Masters degree.

CONTRIBUTORS AND FUNDING SOURCES

This work was supervised by a committee consisting of Professor Krishna Narayanan [advisor] and Professors Jean-Francois Chamberland and Sebastian Hoyos of the Department of Electrical and Computer Engineering and Professor Theodora Chaspari of the Department of Computer Science and Engineering. All work for the thesis was completed independently by the student.

TABLE OF CONTENTS

Page

LIST OF FIGURES

FIGURE Page

1. INTRODUCTION

1.1 Coexistence of Radar and Communication Systems

In recent years there has been a significant increase in the number of radio frequency (RF) devices and this number is projected to increase further in the near future. The current Internet of Things (IoT) boom and the ever increasing amount of data required by smartphone applications are creating a significant load on the existing infrastructure. This load is expected to increase further with the increase in number of devices (as shown in Figure 1.1), causing heavy wireless interference, congested channels and reduced data rates for users.

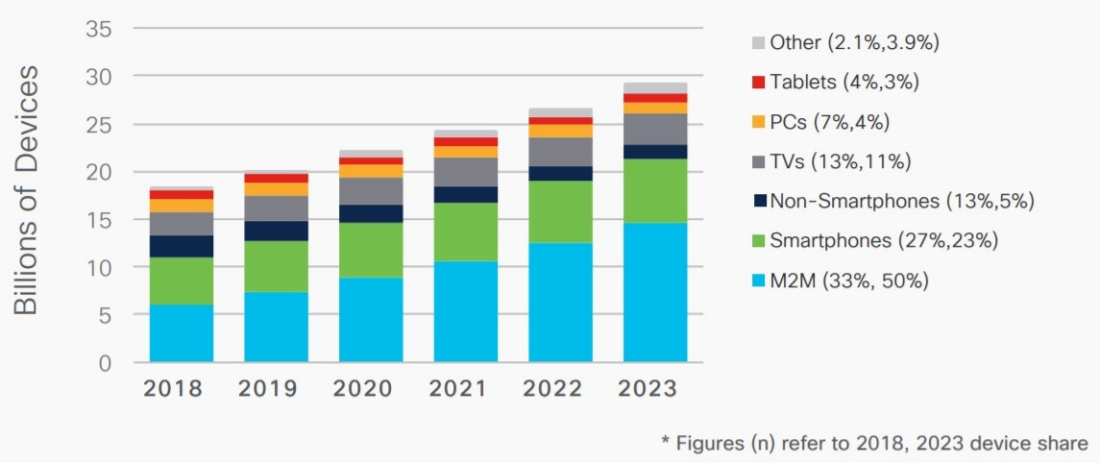

Figure 1.1: Global device growth forecast. Retrieved from [1].

As the RF spectrum becomes more congested, efficient utilization of the available spectrum has become important. Coexistence of radar and communication systems is one approach for increasing the efficiency of spectrum utilisation. Radar systems in general, do not utilise the allocated spectrum all the time during their operation, which leaves a considerable part of the spectrum under utilised. Designing radar and communication systems which can coexist can considerably increase efficiency in utilising the spectrum. Considering the increasing demand for bandwidth,

federal agencies decided to allow commercial communication systems to share the 3550 - 3650 MHz band with military radar systems. This further increased research in this area[2][3].

The core problem of coexistence of radar and communication systems boils down to the handling of interference caused by one system to the other. This problem can be viewed from three different perspectives. The first one is from the perspective of the radar system where the communication signals are treated as interference [4][5], the second one is from the perspective of the communication system where the radar signals are viewed as interference [6, 7] and the third is from a joint perspective where both the systems are jointly designed [8][9]. From the literature, the various solutions can be categorised into three approaches. The first approach is to schedule the transmission in order to prevent or limit interference [10][11][12], the second approach is to design signals in order to avoid interference[13][14][15] and the third approach is to design receivers in order to mitigate interference[16][3][17].

In this thesis, we view the problem of coexistence from the perspective of the radar system and focuses on the third approach of designing a receiver to mitigate interference. The existing radar detector algorithms rely primarily on matched filtering for radar signal detection. These matched filtering based algorithms like Constant False Alarm Rate (CFAR) detector suffer significant detection losses under communication interference [18]. In order to solve this problem, a machine learning based approach is proposed in this thesis. The main motivation for this approach was to solve the problem of communication interference in the radar system without making any changes to the transmitter. Another motivation was to understand if a machine learning algorithm can outperform a matched filter for mitigating interference.

The remainder of this thesis is organised as follows. Chapter 2 presents background on radar systems and neural networks which form the basis for the work done in this thesis. In Chapter 3, the baseline radar detector algorithm is introduced and it's performance is analysed. In Chapter 4 , the Neural Network architectures explored are presented and their performance is evaluated. Lastly, Chapter 5 consists of research conclusions and potential future work.

2. BACKGROUND

2.1 Radar Systems

Radar is an acronym for Radio Detection and Ranging. Radar systems are commonly used for detecting objects and determining their range, velocity, angular position or other characteristics. A radar transmitter transmits a waveform in the direction in which it wishes to measure the presence of an object. The radar receiver receives noise, reflections of the transmitted wave from the environment (clutter) and a reflected wave from the object, if present. These received signals are analysed by the receiver to detect the presence of an object and estimate it's range, velocity etc. The time delay between transmitted and received signal can be used to estimate the range and the Doppler shift produced in the received signal can be used to determine the velocity of the object.

Radars can be classified into many types depending on their application, range, waveform used etc. Based on the application a radar can be classified as ground based, ship based, airborne or space-borne. Depending on the waveform used radar systems can be classified into Continuous Wave (CW) or Pulsed radars. CW radars continuously transmit electromagnetic energy and hence have separate antennas for transmission and reception. The waveforms of CW radars can be pure sine waves and the received echo signals will be centered about a center frequency if stationary objects were present or will be shifted by a Doppler frequency if non-stationary objects were present. This enables CW radar systems to determine the velocity and angular position of the object with great accuracy. But due to this continuous nature of transmission, time delay between signals is essentially zero and hence estimating the range becomes nearly impossible for an unmodulated waveform. To determine the range of objects using CW radars, the signals need to be modulated to have some measure of time delay between the transmitted and received signals.

Unlike CW radars, Pulsed radars have a single transmit and receive antenna. These systems transmit a train of pulsed waveforms (which are usually modulated) through the antenna and then switch to a reception mode for some fixed time after which the next pulse is transmitted. The time

interval between the transmission of two pulses is known as the pulse repetition interval (PRI) and the frequency at which the pulses repeat is known as pulse repetition frequency (PRF). Pulsed radars with low PRF can detect objects at a greater range, where as radars with high PRF can measure the velocity of the objects with greater accuracy. In this thesis, Pulsed radar systems are considered for the problem of radar signal detection.

2.1.1 Pulsed Radar Systems

A Pulsed radar system consists of 4 key components namely the transmitter, duplexer, antenna and receiver (Figure 2.1). The transmitter generates the modulated signal and sends it to the antenna. The duplexer enables the use of a single antenna for both transmission and reception by switching the antenna between the transmitter and receiver. The receiver hardware down-converts the received signal from passband to baseband and processes the baseband signals to determine the range , velocity and other characteristics [19].

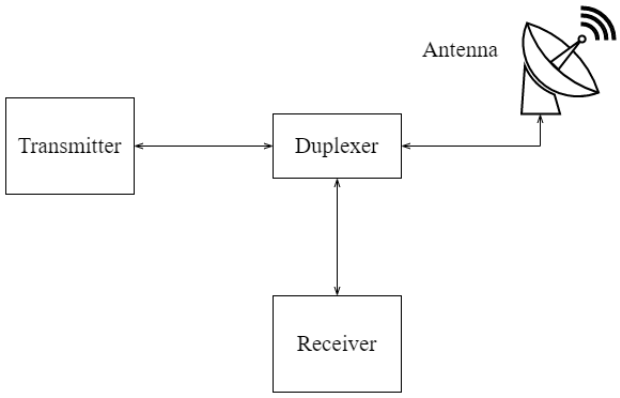

Figure 2.1: Pulsed radar system

The range (R) of the target can be computed from the time delay (τ) between the transmitted and received signal. Since radio waves travel at the speed of light ($c = 3 \times 10^8$m/s), the range of the target can be calculated as shown in Equation 2.1.

$$R = \frac{c\tau}{2} \tag{2.1}$$

The Pulse repetition interval (PRI) is an important characteristic as it determines the maximum unambiguous range of the radar which is the maximum distance at which a target can be located by the radar. Longer PRI or lower PRF allows for detecting farther objects, but would be bad for tracking non stationary targets (especially if it is moving with greater velocity). The width of the transmitted pulse (T) is another important characteristic of the radar as it influences the range resolution of a radar. Range resolution (ΔR) is a quantity that describes the ability of a radar to distinguish between two adjacent objects and is given by

$$\Delta R = \frac{cT}{2} = \frac{c}{2B} \tag{2.2}$$

where B is the bandwidth of the radar signal. Radar systems with shorter pulse width have better range resolution but shorter pulse width would lead to difficulty in estimating the Doppler shift of the received signal [19]. Thus pulsed radar systems with low PRF and short pulse width are suitable for applications where range determination is important whereas systems with high PRF and long pulse width are suitable for applications where velocity determination and tracking are important.

For ranging purposes pulsed radar systems have two requirements which a signal needs to meet in order to be used for transmission.

- The first requirement is that the pulse duration (T) of radar signal needs to be as small as possible as this would result in better range resolution (ΔR).
- The second requirement is that the energy of the signal needs to be high to facilitate longer distance transmission.

Considering these two requirements an impulse signal would be an ideal choice. But in practice signals of short duration and high energy require very high electrical power for transmission as

the power required is equal to the energy of the pulse divided by the length of the pulse. So in order to have signals with high energy the duration of pulse needs to be long. A work around to achieve both these requirements in practice is to transmit a high bandwidth/ low pulse width signal and employ a pulse compression technique at the receiver. Chirp signal combined with a matched filter at the receiver also known as the chirp radar [20] is a popular technique used to meet these requirements.

2.1.2 Chirp Signal

The chirp signal or Linear Frequency Modulated signal is a popular signal used in pulsed radar systems. A chirp signal can be obtained by modulating the frequency of a sinusoidal wave to increase or decrease linearly with time. The Figure 2.2 shows a typical chirp signal.

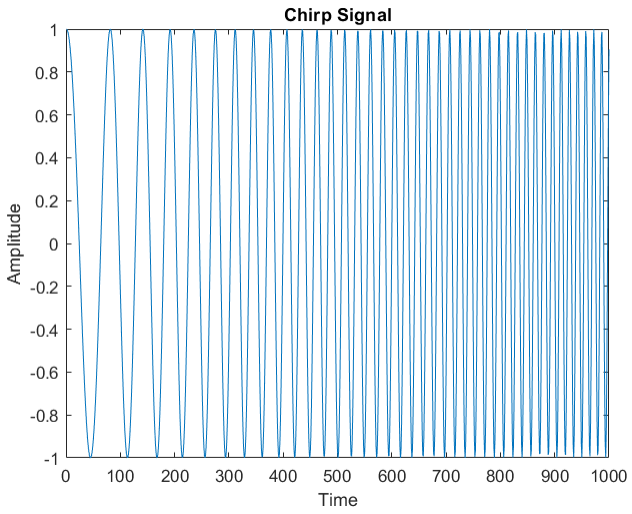

Figure 2.2: Typical chirp signal

Chirp signals are used because of their high bandwidths as this leads to better range resolution

of the radar. A chirp signal of pulse duration T is given by

$$c(t) = \begin{cases} \cos(2\pi(\beta_1 + \beta_2 t)t) \; 0 \leq t \leq T \\ 0, \text{ otherwise} \end{cases} \tag{2.3}$$

where β_1 is the starting frequency of the chirp and $2 \times \beta_2$ is the chirp rate or the rate at which the frequency of the chirp increases. The instantaneous frequency of a chirp signal is given by

$$f(t) = \beta_1 + 2\beta_2 t. \tag{2.4}$$

2.1.3 Matched Filters For Radar

Matched Filters have been widely used for signal detection problems due to their optimality when detecting a signal in the presence of additive white Gaussian noise (AWGN). Given a deterministic signal in white Gaussian noise, one can maximize the signal to noise ratio (SNR) at the receiver by using a filter matched to the signal. Another reason matched filters are used in pulsed radar systems is because of their pulse compression property. When a matched filter is used at the receiver and the signal transmitted is a chirp signal , the output is compressed by a factor of $B\tau$ where B and τ are the bandwidth and pulse duration respectively. The figure 2.3 shows the matched filter output of a chirp signal.

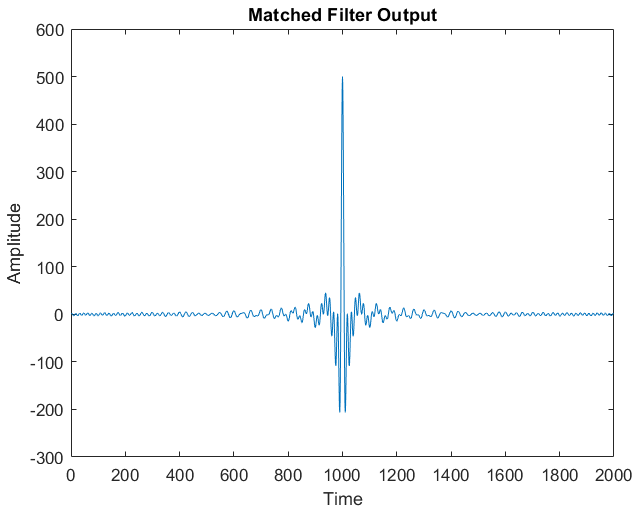

Figure 2.3: Matched filter output for a chirp signal

This compressed pulse obtained from the matched filter allows for better range resolution while enabling long distance target detection.

For the problem of detecting a radar signal in presence of communication interference the use of matched filters or matched filter based techniques will cease to be optimal because of the interference being non white Gaussian. Any in-band interference can lead to deterioration of the detection performance. This non-optimality of the matched filter raises questions regarding the existence of filters which can outperform matched filter under non white Gaussian noise. This aspect is primarily explored in the thesis.

2.2 Neural Networks

Neural networks have been remarkable in pattern recognition and have shown exceptional results in areas like computer vision , natural language processing , voice recognition etc. They are also being experimented in various other fields including wireless communications [21][22][23]. Learning based techniques have also been used for problems like gravitational wave detection [24] and target detection in hyperspectral imagery [21] which rely heavily on matched filter based detection, to overcome the non-optimality of matched filter under non white Gaussian noise.

2.2.1 Neural Network Models

A neural network can be considered to be a directed graph with the neurons as nodes of the graph and the links between the neurons as edges of the graph. A neuron which is the basic computing unit of the neural network, computes an output by applying an activation function to the weighted sum of the inputs (as shown in Figure 2.4). The activation function used plays a significant role in the performance of the network and is usually non-linearity like sigmoid, tanh or Rectified Linear Unit (ReLU) function.

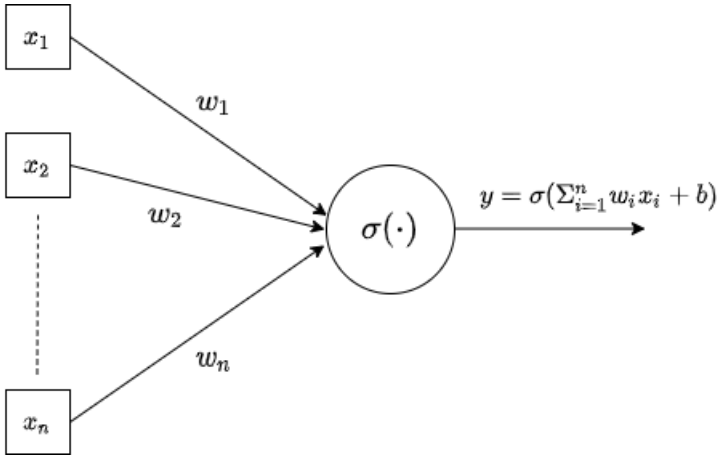

Figure 2.4: A single neuron

The arrangement of the neurons and the links between them gives rise to different models and architectures. In this section, we shall review some models which are relevant to the problem at hand.

2.2.2 Fully Connected Neural Network

A Fully Connected Neural Network (FCNN) also known as a Feed Forward neural network or a Dense neural network is the quintessential model of a neural network. The neurons of this network can be considered to be organised in the form of layers for better understanding of the architecture. The network consists of an input layer , an output layer and multiple hidden layers.

Unlike the other layers, the input layer does not perform any computations (no activation) and is just present to relay the input to the next layer. The number of hidden layers differ from one network to another depending on the complexity of the problem to be solved. The connections between neurons are such that every neuron of one layer is connected to every other neuron of the next layer but the neurons of the same layer are not connected with each other. The activation functions of the neurons need not be the same for all the layers and can be different for different layers of the same network. The architecture is shown in Figure 2.5

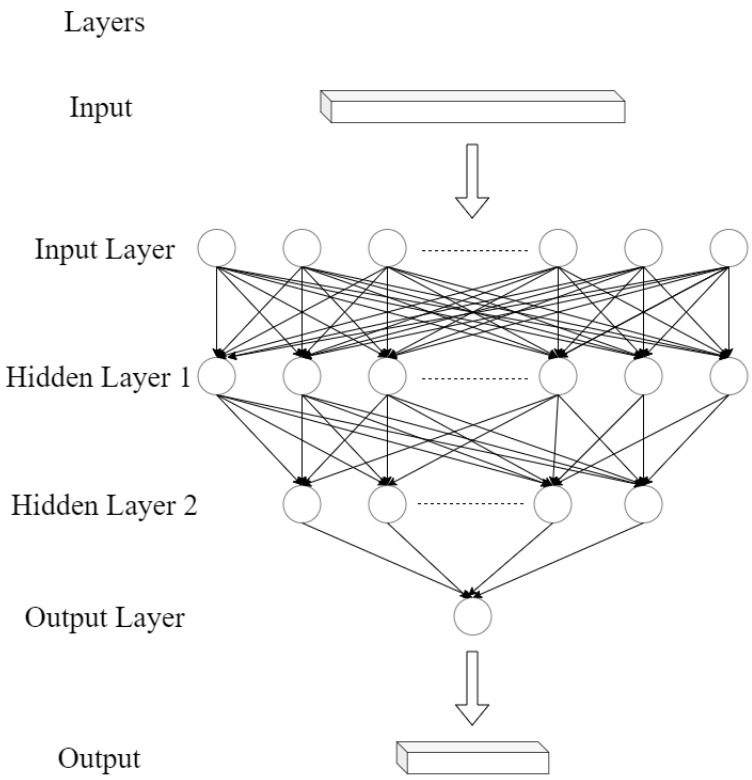

Figure 2.5: Fully connected neural network

An input to such a neural network is passed forward from one layer to another and hence the name feed forward network.

2.2.3 1-Dimensional Convolutional Neural Networks

A Convolutional Neural Network (CNN) is a prominent neural network model developed for image processing applications. CNNs are essentially neural networks which perform convolutions in place of general matrix multiplications in at least one of the layers. CNNs require fewer parameters than fully connected layers and are able to extract meaningful features. CNNs have shown exceptional performance in computer vision problems .

1D CNNs are the 1 Dimensional equivalent of CNNs. They are, in principle, similar to regular CNNs and were designed for analysis of time series data, analysis of signal data over a fixed length period and for Natural Language Processing applications. A CNN is made of 3 essential layers namely, the convolutional layer, the pooling layer and the fully connected layer as output layer. The input to a 1D CNN is a 2D grid with one axis representing time steps and the other axis representing the vector being considered in a time step. For example the time series data of an accelerometer sensor is a 2 dimensional data which consists of a vector of length three which are the x, y and z axis values of the sensor, per time step.

A convolutional layer in a 1D CNN convolves multiple filters across the temporal dimension of the input data to obtain another 2D grid of data as output. The size of the filter can only be varied along one axis which is the time (steps) axis and is fixed along the other axis to be equal to the entire length of the vector. For an input with the shape (no of time steps, length of vector) the output of a convolutional layer would have the shape ($\frac{\text{no of time steps - filter width + 1}}{\text{stride length}}$, no of filters) where stride length is the number of time steps the filter needs to move after every computation. The convolutional operation of a single filter is shown in Figure2.6

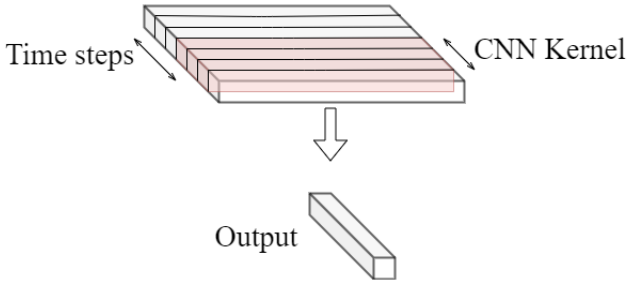

Figure 2.6: 1-D convolutional neural network

The next layer commonly used is the pooling layer which is a method of down sampling the data. The commonly used types of pooling are max pooling or average pooling where a cluster of data are combined by computing the maximum value or performing an average. Finally, a fully connected layer is used to calculate the output vectors (usually probabilities).

2.2.4 Long Short Term Memory

Recurrent Neural Networks (RNNs) are a special class of neural networks whose architecture can be considered as a directed graph with loops. The loops in the network allow for memory to persist and help to capture patterns across the time steps of the input data. The architecture of an RNN can be understood as multiple copies of the same network being applied to different time steps, with connections going from the network copy of one time step, to the copy of the next time step (as shown in Figure2.7).

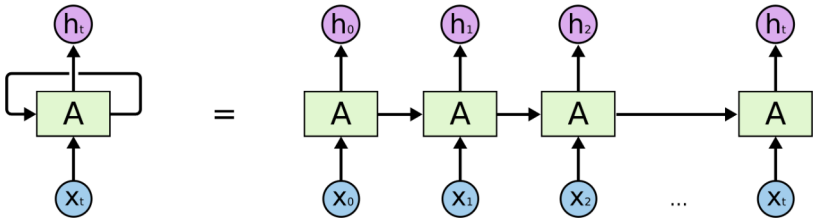

Figure 2.7: Recurrent neural network unrolled

In theory, RNN's should be able to detect dependencies in arbitrarily long sequences, but in practice the back propagation of error vectors through time steps results in either the vanishing gradient or exploding gradient phenomenon. In order to address this problem, a special kind of RNN known as Long Short Term Memory (LSTM) networks were introduced [25]. RNN's have the form of a chain of repeating units, with the repeating unit being a simple structure like a single layer of neurons with tanh activation. Whereas, the repeating units of the LSTMs have 4 layers of neurons with their outputs combined in a unique fashion.

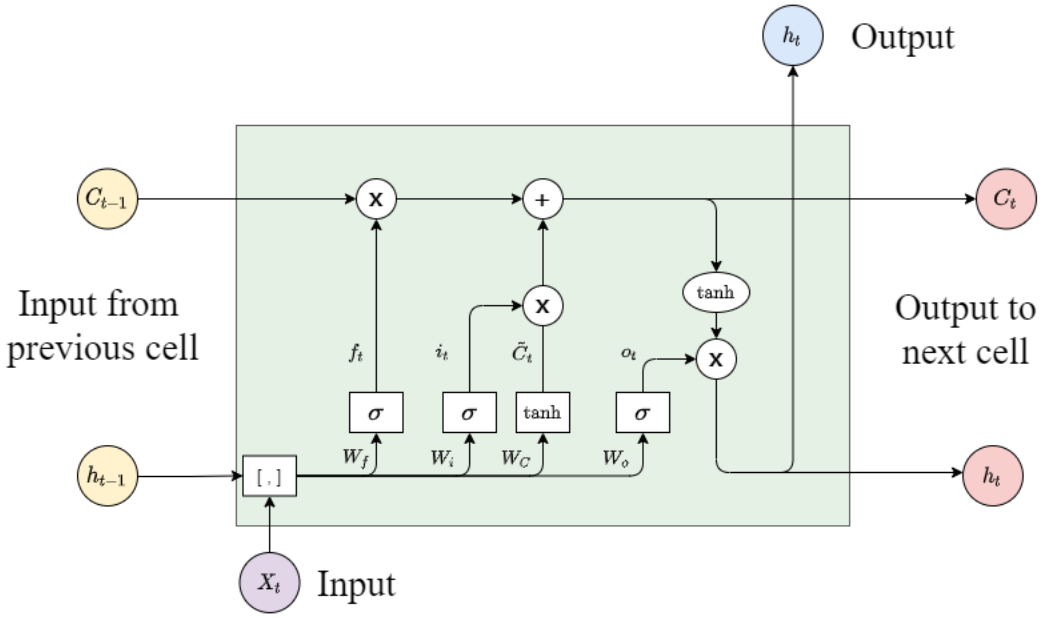

Figure 2.8: A single LSTM cell

As shown in Figure 2.8 an LSTM cell takes in three input vectors X_t, C_{t-1}, h_{t-1} and produces two output vectors C_t and h_t. X_t is the input for the current time step, C_{t-1} is the cell state/ memory from the previous LSTM cell and h_{t-1} is the output of the previous LSTM cell. The output vectors C_t and h_t are the cell state and output vector of the current cell respectively. The operations of performed in a single cell can be given by the Equations 2.5 - 2.10

$$f_t = \sigma(W_f \cdot [h_{t-1}, X_t] + b_f) \tag{2.5}$$

$$i_t = \sigma(W_i \cdot [h_{t-1}, X_t] + b_i) \tag{2.6}$$

$$\tilde{C}_t = \tanh(W_C \cdot [h_{t-1}, X_t] + b_C) \tag{2.7}$$

$$C_t = f_t \cdot C_{t-1} + i_t \cdot \tilde{C}_t \tag{2.8}$$

$$o_t = \sigma(W_0 \cdot [h_{t-1}, X_t] + b_0) \tag{2.9}$$

$$h_t = o_t \cdot \tanh(C_t) \tag{2.10}$$

The Cell state (C_t) and its propagation are significant in understanding the functioning of an LSTM cell. The output of previous layer (h_t) and the current input (X_t) are concatenated to form the input for the 4 neural network layers in the cell. The cell state vector from the previous LSTM cell (C_{t-1}) is multiplied element wise with the vector obtained from the first sigmoid layer (f_t). The first sigmoid layer is known as the forget gate. Since the sigmoid function outputs values between 0 and 1 the vector f_t when multiplied element wise with C_t would just regulate the elements of C_t, which would mean that the output from the forget layer essentially dictates what elements from the previous cell state shall be forgotten and what shall be remembered. The second sigmoid gate is known as the input gate and it regulates the new candidate cell state vector ($\tilde{C}_t$) obtained from the output of the tanh layer. The weighted previous cell state and the weighted candidate cell state are added to obtain the current cell state. The last sigmoid gate is known as the output gate and it's output vector (o_t) regulates the candidate output. The candidate output is obtained by passing the cell state through a tanh function and this when multiplied with the vector from the output gate yields the current output vector (h_t). Hence through the process of training, an LSTM cell learns to regulate the previous cell state, candidate cell state and candidate output in order to produce the current cell state and output.

3. BASE LINE ALGORITHM: CONSTANT FALSE ALARM RATE (CFAR) DETECTOR

3.1 Model

For our problem of radar signal detection the received signal $r(t)$ at the radar can be considered as a sum of three components which are the radar signal (signal of interest), communication signal (interference) and AWGN noise, given by

$$r(t) = s(t) + z(t) + n(t) \tag{3.1}$$

The radar signal here is considered to be a chirp signal of pulse duration T, given by

$$s(t) = \begin{cases} \cos(2\pi(\beta_1 + \beta_2 t)t) \; 0 \leq t \leq T \\ 0, \text{ otherwise} \end{cases} \tag{3.2}$$

where β_1 is the starting frequency of the chirp and $\frac{\beta_2}{2}$ is the chirp rate. The communication interference is assumed to be a Quadrature Amplitude Modulated (QAM) signal and is given by

$$z(t) = \sum_k x_i[k]p(t - kT_c)\cos(2\pi f_c t) - x_q[k]p(t - kT_c)\sin(2\pi f_c t) \tag{3.3}$$

where $x_i[k]$ and $x_q[k]$ are the real and imaginary parts of the k^{th} QAM symbols drawn from an M-ary alphabet and f_c is the carrier frequency. The noise $n(t)$ is considered to be additive white Gaussian noise (AWGN). Considering that the radar signal component would be a time delayed and reflected version of the chirp signal, the received signal for the time interval $0 \leq t \leq T$ is given by

$$r(t) = \sqrt{P_s} \cdot s(t - \tau) + \sqrt{P_i} \cdot z(t) + n(t) \tag{3.4}$$

where τ is the time delay of the chirp signal and P_s, P_i are signal power and interference power, respectively. The pulse repetition interval of the radar is t_p seconds. The received signal is then

down-converted and sampled every T_s seconds to obtain samples of the baseband signal $r[n]$. The objective of the radar receiver is to detect if a signal is present or not and to estimate the range of the target with high accuracy.

3.2 Baseline: Cell Averaging Constant False Alarm Rate Receiver

The Constant False Alarm Rate (CFAR) Detector is a popular adaptive algorithm used for radar detection. The CFAR technique helps to adaptively determine the power threshold above which a signal is considered to be present. An extremely low threshold can lead to a high probability of false alarm and a very high threshold leads to a low probability of detection. Hence the threshold has to be set by balancing this trade off.

The cell averaging CFAR (CA-CFAR) is a commonly used CFAR algorithm. In this algorithm the received signal is first divided into cells (bins) each of length $T + \tau_{max}$. It is assumed that the maximum possible delay (τ_{max}) is known to the receiver. Each cell consists of the received signal from time kT to $kT + \tau_{max}$. Hence there is an overlap of signal for duration τ_{max} in adjacent cells. At a given point, the CA-CFAR detector tries to detect the presence of a radar signal in one cell. This cell is referred to as the Cell Under Test (CUT).

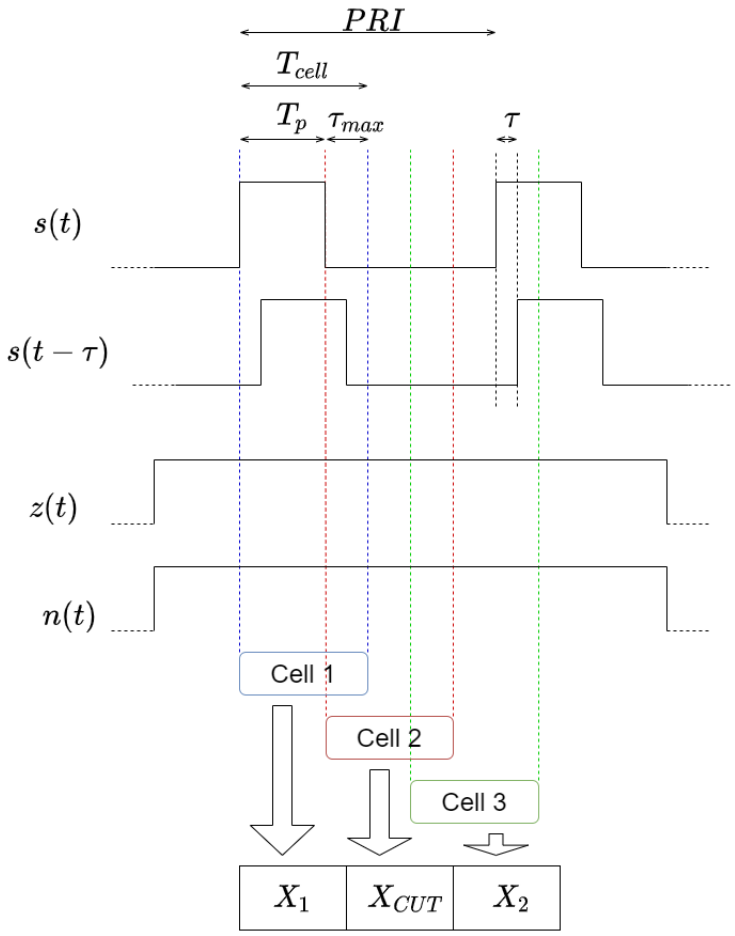

Figure 3.1: CFAR algorithm

The Figure 3.1 visualises the CFAR algorithm for the signal model of this problem. The presence of the radar is detected by comparing the energy of the matched filter output of the CUT (X_{CUT}) with the average energy of the matched filter outputs of the number of neighbouring cells (X_i). The detector is given by

$$\hat{Y} = \begin{cases} 1, \ |X_{CUT}|^2 > \lambda \cdot \frac{1}{N_{cell}} \sum_{i=1}^{N_{cell}} |X_i|^2 \\ 0, \ |X_{CUT}|^2 \leq \lambda \cdot \frac{1}{N_{cell}} \sum_{i=1}^{N_{cell}} |X_i|^2 \end{cases} \tag{3.5}$$

here λ is a threshold constant used to control the probability of false alarm and the optimum value of λ varies with respect to the SNR of the system , the number of cells and the pulse repetition

frequency.

While this algorithm is optimal for detecting signals with AWGN noise, its performance is not optimal in the presence of non-Gaussian noise, i.e., interference $z(t)$.

3.3 Signal Generation Parameters

In this section, the parameters of the received radar signals used for the evaluation of the performance of CFAR detector are presented. For signal generation the receiver structure shown in Figure 3.2 is assumed.

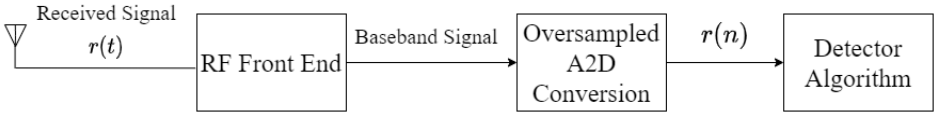

Figure 3.2: Receiver structure

Under this structure the radar receiver down converts the passband received signal $r(t)$ to a baseband version. This baseband version is then sampled to convert the analog signal to a digital version $r(n)$. This sampled baseband version of the received signal is used by the detector algorithm. Hence, for testing the detector performance, only the received signals $r(n)$ are generated using parameters similar to a baseband level operation. Without loss of generality the sampled baseband received signal is considered to be the sum of sampled baseband versions of the radar signal, QAM interference signal and AWGN signal. It is also considered that the CFAR receiver knows the maximum possible time delay (τ_{max}).

The performance of the CFAR detector was evaluated for two types of interference which are narrow band interference and wide band interference. For narrow band interference the symbol rate of the QAM signal should be lesser than the start frequency of the chirp signal whereas for wide band interference the symbol rate of the QAM signal should be greater than the start frequency of the chirp. Interference power and SNR are the varying parameters for evaluating the detector's

performance. The interference power is a constant whose square root (amplitude) is multiplied to the interference signal to vary it's power. The SNR is given by,

$$SNR = 10\log_{10}\left(\frac{E_s}{N \times \sigma^2}\right) \tag{3.6}$$

where E_s is the energy of the discrete-time signal and σ^2 is the noise variance.

Two sets of parameters were considered for signal generation, while the first set of parameters were chosen purely from a detection point of view the second set of parameters were chosen considering the ranging abilities of the radar. For both the sets of parameters, a dataset of 10,000 received signals were generated for each configuration of SNR and interference power. These datasets were used for evaluating the performance of the detector for that configuration.

3.3.1 First Set of Parameters

The first set of radar system parameters are given in Table 3.1.

PARAMETER	VALUE
Sampling Frequency - F_s	10 MHz
Sampling Time - T_s	0.1μs
Maximum possible time delay - τ_{max}	2 μs $\equiv$ 20 samples
No of cells	3
Radar signal power - P_s	1
Start frequency of chirp signal - β_1	0.1 MHz
Chirp rate/2 - β_2	3 MHz/s
Pulse Duration - T	0.1 ms $\equiv$ 1000 samples
Bandwidth - BW	600 Hz
Time Delay - τ	(0.1μs - 2.0μs) $\equiv$ (1 - 20) samples
Cell Duration - $(T + \tau_{max})$	102 μs $\equiv$ 1020 samples

Table 3.1: Radar system parameters (Set 1)

The sampling frequency was selected such that the radar signal is over sampled . The length of cell is fixed at 1000 samples due to computational constraints. The signal power of the radar is fixed at 1. The parameters of the interference signal are given in Table3.2 .

PARAMETER	WIDE BAND	NARROW BAND
Carrier Frequency - f_c	100 MHz	0.1 MHz
Symbol Rate	1 MHz	10 KHz

Table 3.2: Interference signal parameters (Set 1)

The interference carrier frequency here is not the actual carrier frequency (which is of GHz

range), but is brought down to a lower frequency range for simulation purposes. The range of SNR and interference power are given in Table 3.6.

PARAMETER	RANGE
SNR	-10dB - 10dB
Wide band interference power	0 - 10
Narrow band interference power	0 - 5

Table 3.3: Variable parameters (Set 1)

The signal components generated from the first set of parameters can be seen in the Figures 3.3 (a) and (b).

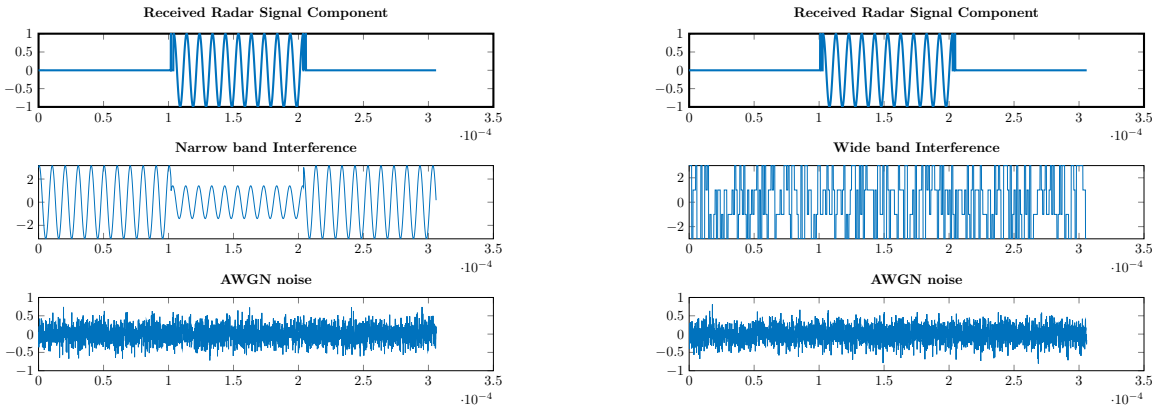

(a) Wide band interference

(b) Narrow band interference

Figure 3.3: Signal components (Set 1)

The first set of parameters have the following issues which makes them unsuitable for radar ranging.

- The chirp signal has very low bandwidth which results in poor range resolution (250 Km).
- The maximum possible range (600m) is much lower than the range resolution of the radar.

3.3.2 Second Set of Parameters

A second set of parameters as shown in Table 3.4 are chosen such that the radar system would be suitable for ranging.

PARAMETER	VALUE
Sampling Frequency - F_s	100 MHz
Sampling Time - T_s	0.01μs
Maximum possible time delay - τ_{max}	4 μs $\equiv$ 400 samples
Minimum simulated time delay	0.5 μs $\equiv$ 50 samples
Maximum possible Range	600m
Minimum simulated Range	75m
No of cells	3
Radar signal power - P_s	1
Start frequency of chirp signal - β_1	1 MHz
Chirp rate/2 - β_2	300 GHz/s
Pulse Duration - T	10 μs $\equiv$ 1000 samples
Bandwidth - BW	6 MHz
Stop frequency of chirp signal	7 MHz
Range Resolution - ΔR	25m
Time Delay - τ	(0.5μs - 4.0μs) $\equiv$ (50 - 400) samples
Cell Duration - ($T_{cell} = T + \tau_{max}$)	14 μs $\equiv$ 1400 samples

Table 3.4: Radar system parameters (Set 2)

The following constraints are met by these parameters

- The pulse duration is fixed at 1000 samples.
- The signal has high bandwidth (6MHz) resulting in great range resolution (25m).
- The range resolution (25m) is lower than the minimum simulated range (75m)

Thus the set of parameters represent a radar system suitable for ranging. The performance of the CFAR detector under this set of parameters is evaluated for an additional narrow band interference case. The second set of interference signal parameters are shown in Table 3.5.

Parameters	Narrow Band 1	Narrow Band 2	Wide Band
Symbols/cell - L	1	2	160
Symbol Rate - f	62.5 KHz	125 KHz	100 MHz
Carrier Frequency - f_c	5 MHz	5 MHz	1 GHz

Table 3.5: Interference signal parameters (Set 2)

The range of SNR and interference power for the second set are given in Table 3.6.

PARAMETER	RANGE
SNR	-20dB - 10dB
Wide band interference power	0 - 100
Narrow band interference power	0 - 10

Table 3.6: Variable parameters (Set 2)

The signal components generated from the first set of parameters can be seen in the Figures 3.4 (a) and (b).

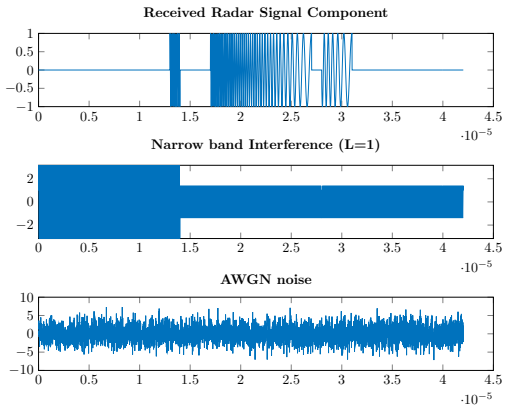

(a) Wide band interference

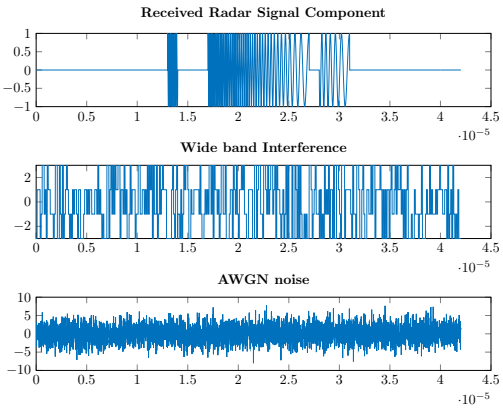

(b) Narrow band interference

Figure 3.4: Signal components (Set 2)

3.4 Results

In this section, the detection performance of the CFAR detector on the signal datasets of the two parameter sets are presented.

3.4.1 First Set of Parameters

The nature of the interference signal can cause a significant impact on the detection performance of the receiver. A clearer understanding can be obtained from the Fourier transform plot of the radar signal and interference signal.

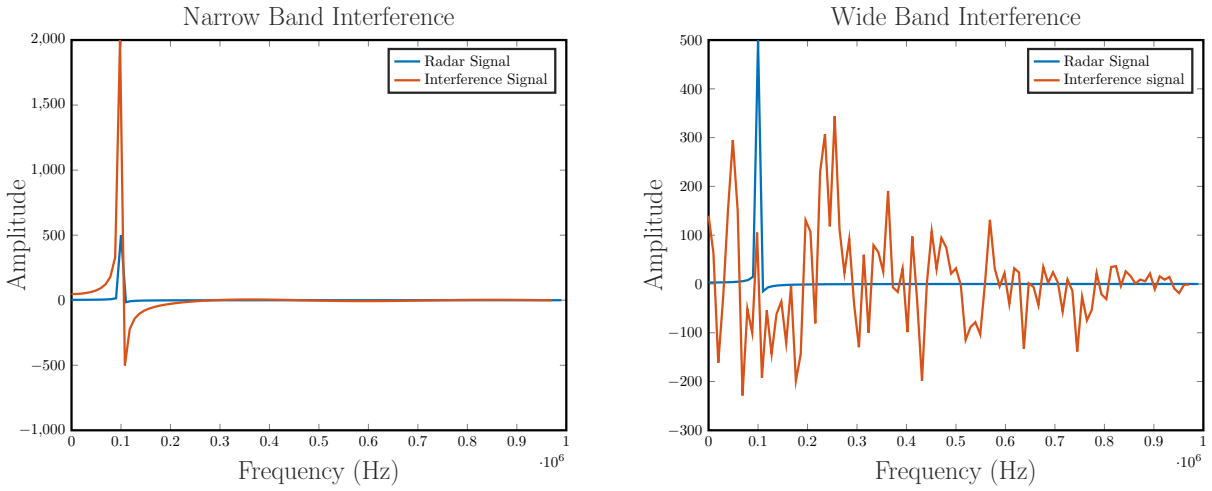

(a) Wide band interference

(b) Narrow band interference

Figure 3.5: Fourier transform of radar signal and interference signal (Set 1)

The Figures 3.5 (a) and 3.5 (b) show the amount of interference which is in the frequency band of radar signal. From the plots, it can be observed that the entire power of the narrow band signal is concentrated in the radar signal's band while the same power is spread across the bandwidth for the wide band signal. Thus for the same power the narrow band interference is a much stronger interference signal to the radar than the wide band signal.

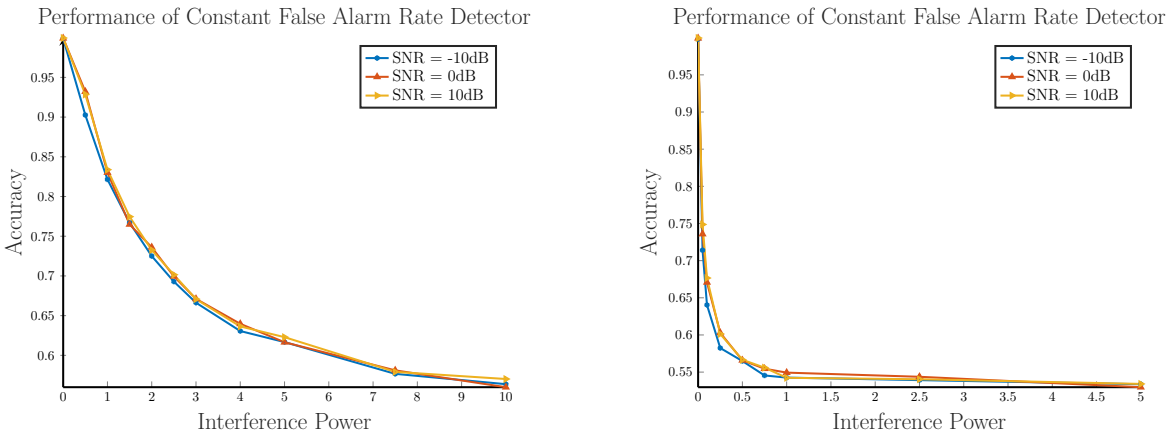

(a) Wide band interference

(b) Narrow band interference

Figure 3.6: Performance of CFAR detector under wide band and narrow band interference for different SNRs (Set 1)

The Figure 3.6 (a) shows the performance of the CFAR detector under wide band interference for different values of SNR. The probability of error for each configuration of SNR and interference power, is computed from 10,000 signals. This plot shows that with increase in interference power, the probability of error of the detector also increases, whereas the increase in SNR causes little to no improvement in the performance of the detector. Thus the degradation of performance can be attributed only to the interference power for the given range of SNRs. Under narrow band interference as observed in Figure 3.6 (b), the performance of the CFAR detector degrades drastically with a slight increase in interference power and the performance does not improve much with the increase in SNR. From the plots it can also be observed that the detector performance under narrow band interference is worse than that under wide band interference, and this can be attributed to the very high in-band interference power of the narrow band signal.

3.4.2 Second Set of Parameters

For the second set of parameters, an additional type of narrow band interference is also considered with greater number of symbols per cell. The Figures 3.7 (a), (b) and (c) show the amount of interference which is in the frequency band of the radar signal.

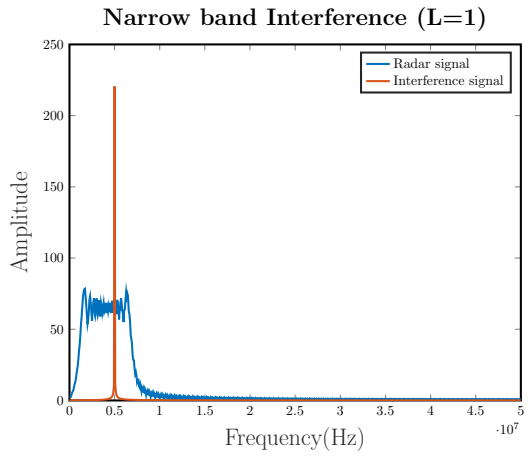

(a) Narrow band interference 1 (L=1)

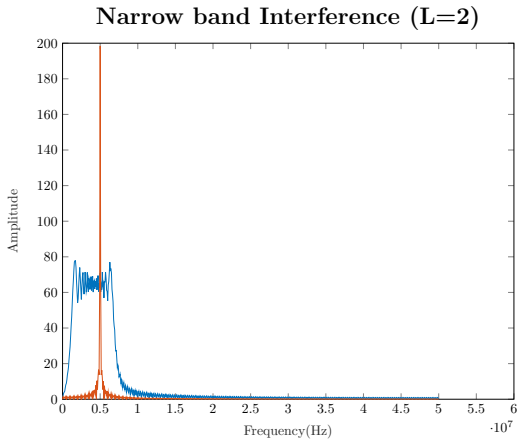

(b) Narrow band interference 2 (L=2)

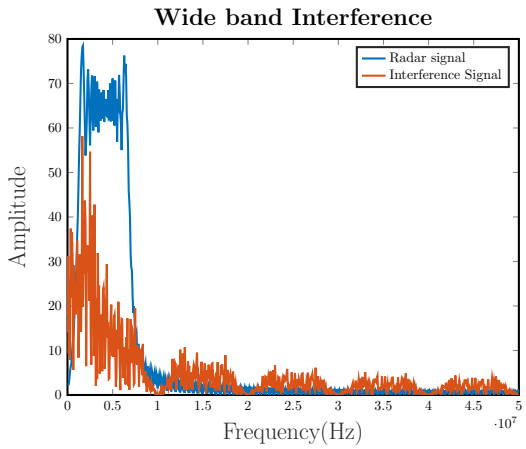

(c) Wide band interference

Figure 3.7: Fourier transform of radar signal and interference signal (Set 2)

It can be observed that the narrow band signals have very high in-band power while the wide band interference has lower in-band power as its power is spread across the bandwidth. The second narrow band interference has slightly wider bandwidth than the first narrow band signal due to greater symbol rate. When compared to the spectrum of the signals under the first set of parameters, the following observations can be made.

- The radar signal occupies a much wider bandwidth.
- The narrow band signals have much narrower spectrum than the radar signal.

- The wide band interference has greater in-band power.

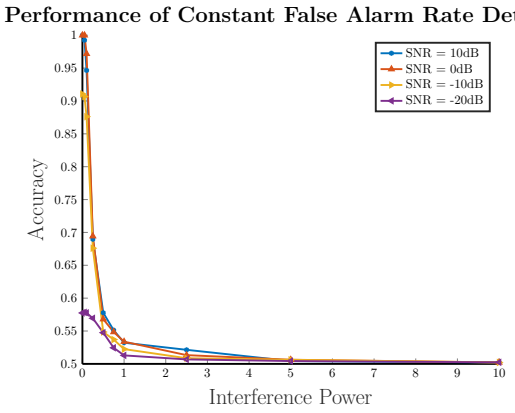

(a) Narrow band interference 1 (L=1)

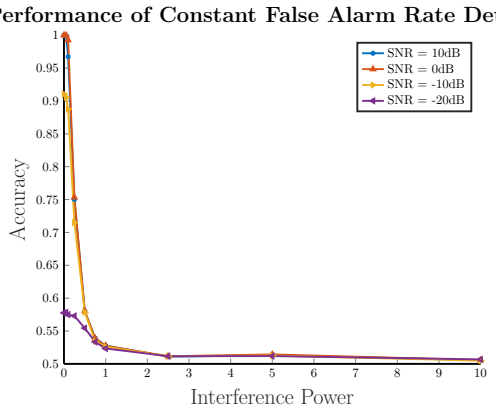

(b) Narrow band interference 2 (L=2)

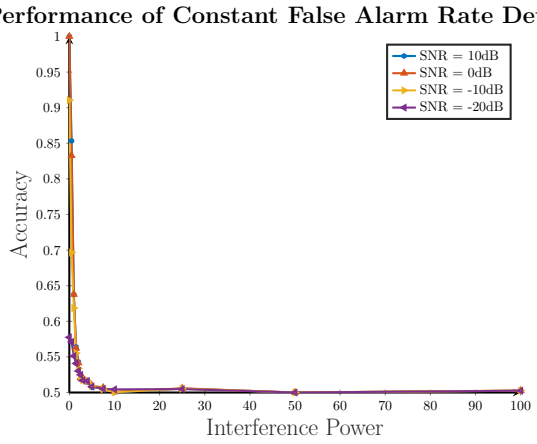

(c) Wide band interference

Figure 3.8: Performance of CFAR detector under wide band and narrow band interference for different SNRs (Set 2)

The Figure 3.8 (a) and (b) shows the performance of the CFAR detector under narrow band interference signals. Under narrow band interference, it can be observed that the performance degrades steeply with the increase in interference power. The performance under both the narrow band cases is poor under -20dB SNR and is almost identical under other SNRs.

The performance of the CFAR detector under wide band interference can be observed from the Figure 3.8 (c). This plot shows that with the increase in interference power, the accuracy of detection decreases and at interference powers greater than 10 the detector performs very poorly. At -20dB SNR the detector performance is poor but at higher SNRs the performance improves for lower interference powers (0-10) while remaining poor for high interference powers. The trend of not improving with increase in SNRs can be seen for high SNRs.

4. NEURAL NETWORK BASED RADAR RECEIVER DESIGN

In this chapter different neural network architectures are explored for solving the radar detection problem. The rationale for applying neural networks to this problem is the fact that communication signals have an underlying structure and the expectation is that neural networks can learn this structure and cancel it out to detect the radar signals. In other words, the neural networks are expected to learn a good function for this hypothesis testing problem.

4.1 Datasets for the Neural Networks

The dataset used for training the neural network is a defining characteristic of the neural network, and it is important that the dataset used exactly reflects the problem at hand. In order to be able to make direct comparisons between the performance of the baseline receiver and the neural network, the input to the neural network was required to be the same as that of the CFAR detector. The CFAR detector model in Section 3.2 divided the received signals into cells of length T (pulse duration)+ τ_{max} (maximum possible time delay) and used matched filters to detect the presence of radar signal in each cell. Hence the radar received signals divided into these cells formed the dataset for the neural neural networks. Just as the CFAR detector, the performance of the neural network based architectures are tested on the two different sets of parameters. The table 4.1 shows the parameters for signal generation

PARAMETER	SET 1	SET 2
Sampling Frequency - f_s	10 MHz	100 MHz
Start frequency of chirp signal - β_1	0.1 MHz	1 MHz
Chirp Rate/2 - β_2	3 MHz/s	300 GHz/s
Pulse Duration - T	0.1 ms $\equiv$ 1000 samples	10 μs $\equiv$ 1000 samples
Bandwidth - BW	600 Hz	6 MHz
Maximum possible time delay - τ_{max}	2 μs $\equiv$ 20 samples	4 μs $\equiv$ 400 samples
Interference Carrier Frequency - f_c (WB | NB1 | NB2)	100 MHz| 0.1 MHz	1 GHz| 5 MHz| 5 MHz
Radar signal power - P_s	1	1
Interference signal power - p_i (WB | NB1 | NB2)	0 - 5|0 - 10	0 - 100|0 - 10|0 - 10
SNR	-10dB - 10dB	-20dB - 10dB
No of Cells	3	3
Cell Duration - $(T + \tau_{max})$	102 μs $\equiv$ 1020 samples	14 μs $\equiv$ 1400 samples

Table 4.1: Signal generation parameters

For each configuration of SNR and interference power a separate dataset was created. Each dataset comprised of 10,000 signals obtained from 3 cells of the baseline receiver model and hence the dimension of the dataset was 10000x3x1020. The 2nd cell among the three cells is the cell under test (CUT) and for half of the dataset had radar signal present in the CUT and in the rest half the radar signal was absent.

4.2 Neural Network Architectures Explored

The problem of radar signal detection can be viewed as a binary classification problem with the presence of radar signal as one class and the absence of radar signal being the other class.

The neural networks designed are expected to learn whether a radar signal is present in the cell under test (CUT) or not. There are an endless number of neural network architectures that can be designed for this problem and in this thesis we explore a few of them. The architectures explored involve a combination of Fully Connected Layers (FCNN), Long Short Term Memory (LSTM) Layers , 1 dimensional convolutional layers (1D CNN).

4.2.1 Fully Connected Neural Network

4.2.1.1 Architecture

In order to get a preliminary understanding of the performance of neural networks for the radar detection problem, a simple Fully Connected Neural Network model with two hidden layers and an output layer was selected. This model was first explored for the single cell case where the network is trained to detect the presence of radar in the CUT without being provided the signals of the adjacent cells. The model was then explored for the three cell case in which the signals in the adjacent cell are provided along with the CUT. The dimensions of the neural network layers for the two cases are given in Table 4.2.

LAYER	SET 1 (Single Cell/Three Cells)	SET 2 (Single Cell/Three Cells)
Input Layer	1020/3060	1400/4200
Hidden Layer 1	1020/3060	1400/4200
Hidden Layer 2	256/1024	256/1024
Output Layer	1/1	1/1

Table 4.2: Dimensions of neural network layers

Since the resulting signals from the two sets of parameters were of different dimensions , separate neural networks with suitable dimensions were designed for each case.

4.2.1.2 Hyperparameters

The hyperparameters fixed for training are given in Table 4.3

HYPERPARAMETER	SET 1	SET 2
Train : Test Data Split	8000:2000	8000:2000
Loss Function	Binary Cross Entropy (BCE)	Binary Cross Entropy (BCE)
Optimizer	Adam	Adam
Learning Rate	10^{-4}	10^{-4}
Learning Rate Decay	10^{-6}	10^{-5}
Batch Size	32	32
Epochs	100	100

Table 4.3: Hyperparameters

Since the classification problem is binary in nature, the Binary Cross Entropy (BCE) loss function was considered to be the most appropriate loss function. The optimizer used was Adam optimiser [26], a popular adaptive gradient descent algorithm. Adam is commonly used in computer vision applications and is considered to be appropriate for noisy problems. Adam algorithm maintains a separate learning rate for every parameter of the network and these learning rates are adapted along the training process. The learning rate parameter specified is the initial learning rate for all the parameters and as the learning rates for the parameters get updated the specified learning rate becomes an upper bound for the updated learning rates. The Learning rate decay is a parameter which reduces the learning rate, which is an upper bound for the updated individual learning rates of the parameters, with every epoch. This ensures that the learning rate remains low towards the end of the epoch. The update of the learning rate (lr) parameter from the old learning rate (lr_old) and the learning rate decay (lr_decay) parameter is given by

$$lr = \frac{lr\_old}{1 + lr\_decay}$$

4.2.1.3 Results

In this section the performance of the FCNN architecture for the single cell case and three cell case is presented. The performance of the architecture is evaluated on signal datasets of the two sets of parameters. The same datasets are used for both the cases but for the single cell case only the CUT is taken as input. The accuracy of the neural network on the test set is used as a measure of its performance.

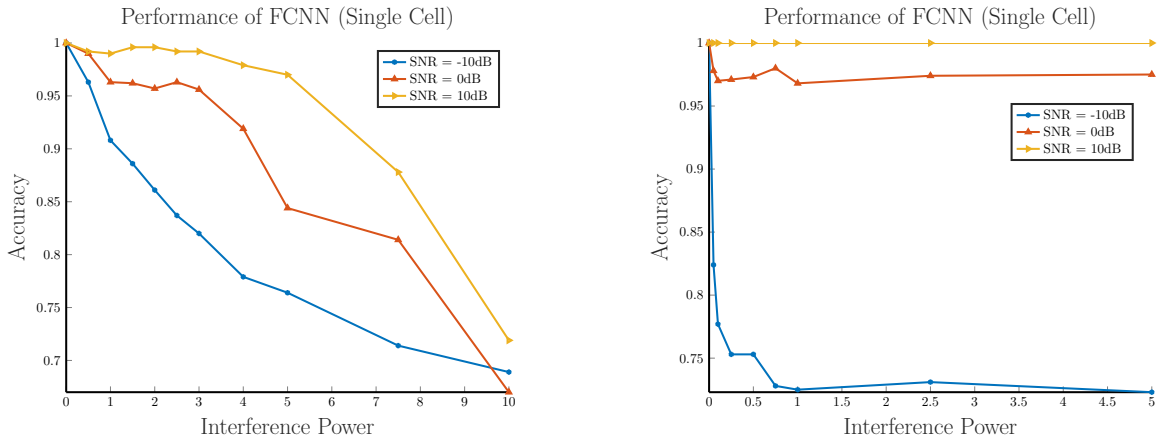

(a) Wide band interference

(b) Narrow band interference

Figure 4.1: Performance of single cell FCNN network under wide band and narrow band interference for different SNRs (Set 1)

The Figure 4.1 (a) shows the performance of the single cell FCNN uder wide band interference for the first set of parameters. A decrease in performance can be observed with increase in Interference power. For low to medium interference power, the increase in SNR appears to improve the detection performance, but for higher interference powers, lesser improvement can be observed. The performance of the architecture for the narrow band interference case as shown in Figure 4.1

(b) appears to be exceptional for high SNRs and a significant improvement of performance can be observed with the increase in SNR.

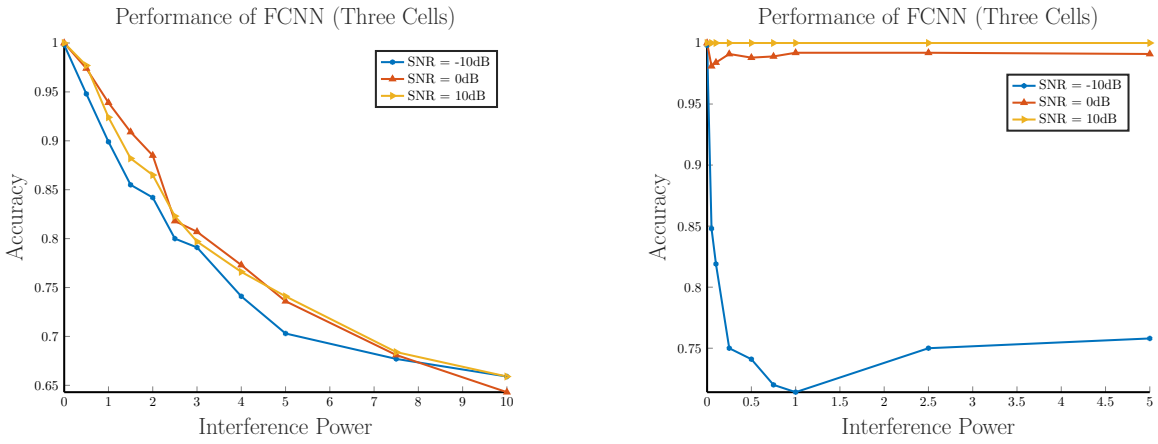

(a) Wide band interference

(b) Narrow band interference

Figure 4.2: Performance of three cell FCNN network under wide band and narrow band interference for different SNRs (Set 1)

The performance of the three cell FCNN architecture under wide band interference for the first set of parameters as shown in Figure 4.2 (a) follows a similar decreasing trend as the single cell architecture , but unlike it the performance of the three cell architecture does not improve significantly with the increase in SNR. The performance under narrow band interference is similar to that of the single cell case with increase in SNR causing a significant improvement to the detection performance.

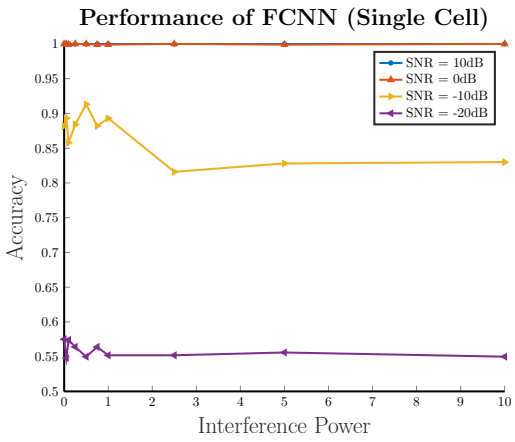

(a) Narrow band interference 1

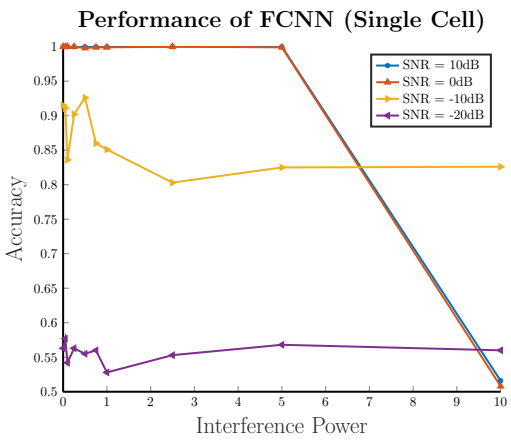

(b) Narrow band interference 2

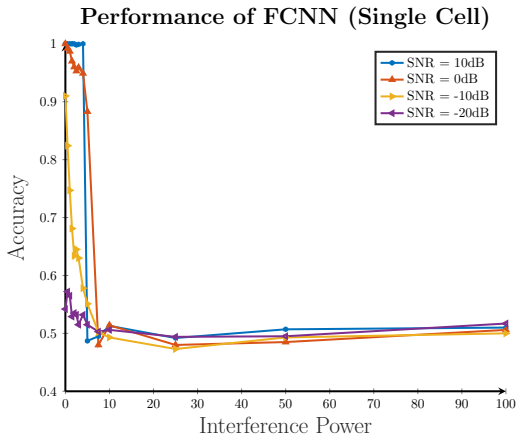

(c) Wide band interference

Figure 4.3: Performance of single cell FCNN network under wide band and narrow band interference for different SNRs (Set 2)

The Figures 4.3 (a) and (b) show the performance of the single cell FCNN architecture under the two types of narrow band interference for the second set of parameters. From the Figure 4.3 (a) it can be observed that at high SNRs the performance is exceptional, and a significant boost in performance can be observed with the increase in SNR. It can also be seen that the performance does not degrade with increase in significantly with the increase in SNR. A similar trend is observed for the second narrow band interference with the exception of an unexpected behaviour at high SNR and interference power of 10 where a drastic decline in performance is observed. The wide band

performance of the architecture can be observed from the Figure 4.3 (c), where the performance degrades with the increase in interference power. The increase in SNR boosts the performance of the network.

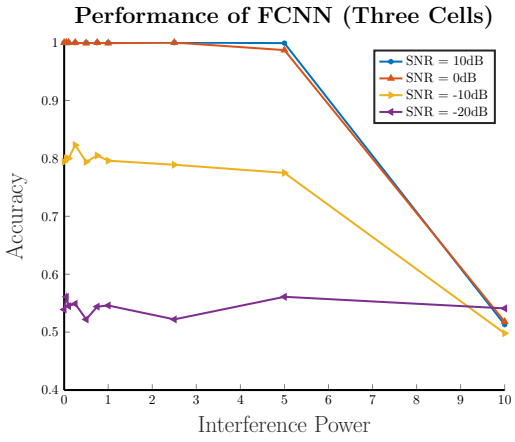

(a) Narrow band interference 1

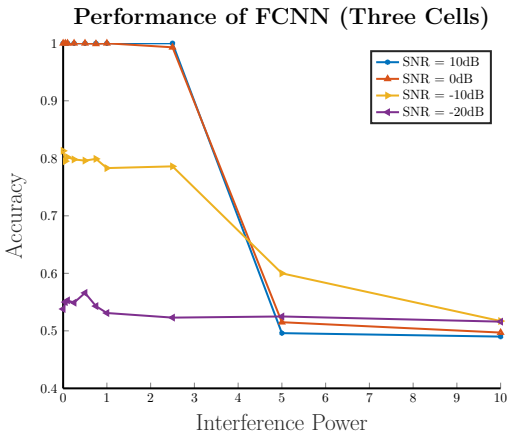

(b) Narrow band interference 2

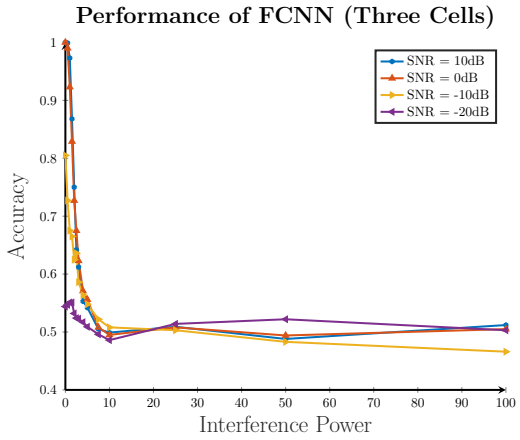

(c) Wide band interference

Figure 4.4: Performance of three cell FCNN network under wide band and narrow band interference for different SNRs (Set 2)

From the Figures 4.4 (a) and (b) the performance of the three cell FCNN architecture under the two types of narrow band interference for the second set of parameters can be seen. Under the first narrow band interference the performance remains almost constant at low interference

powers (< 5) and interference power 10 the performance appears to drastically drop under all SNRs. Under the second narrow band interference the performance degrades at interference power 5, while it remains almost constant at lower powers. For both the interference cases a boost in performance with increase in SNR can be observed for lower interference powers. The wide band performance of the network as shown in Figure 4.4 (c) appears to gradually degrade with increase in interference power and a performance improvement can be observed with the increase in SNR at lower interference powers (<10).

4.2.2 Time Distributed FCNN - LSTM

4.2.2.1 Architecture

In this section, we present an architecture which uses a combination of Time Distributed Fully Connected layers and LSTM layers. The time distributed wrapper allows for applying a single neural network layer to multiple time steps of the data. Considering a neural network layer as a filter, applying a time distributed layer is similar to applying the same filter to the different time steps of the input. Unlike RNNs in which the output of one time step influences the outputs of the next time steps, here the outputs of the time steps are independent, but the weights of the layer are learned considering all the time steps. The Figure 4.5 visualises the network architecture.

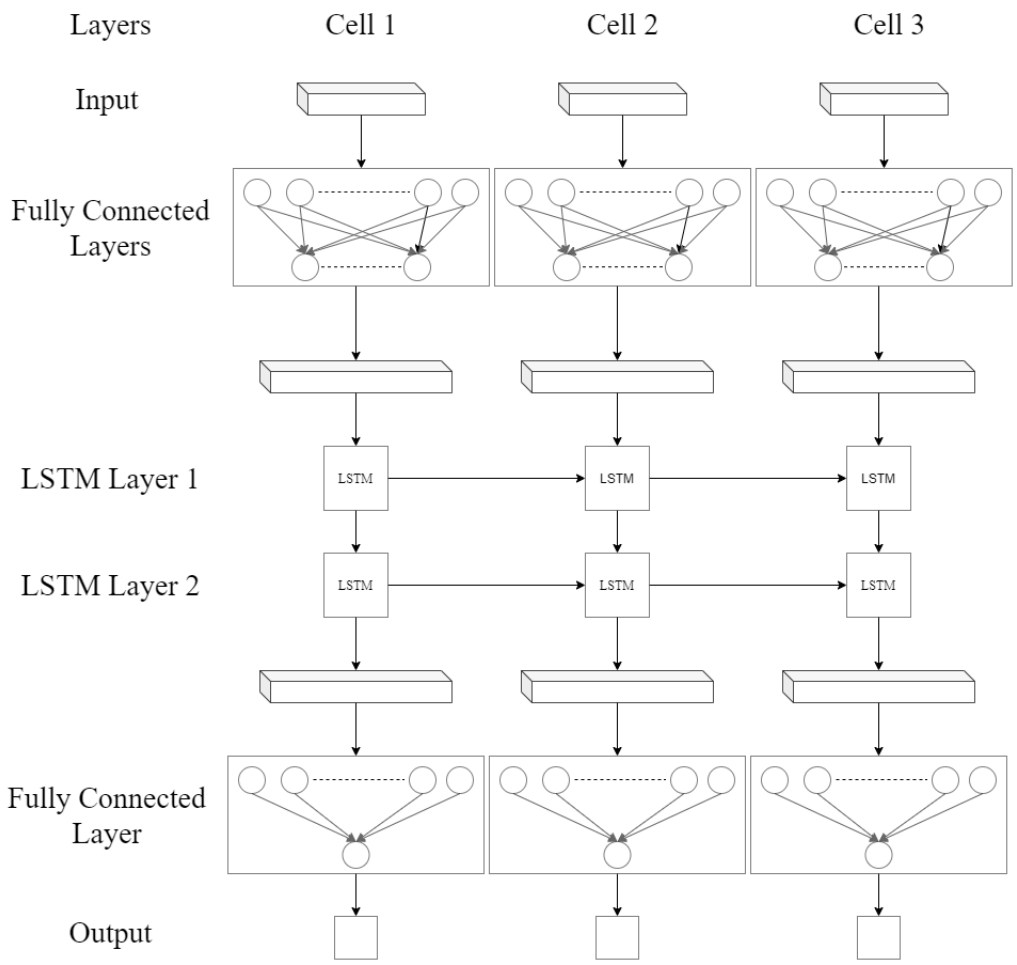

Figure 4.5: Time Distributed FCNN - LSTM architecture

While the visualisation shows three different FCNNs it is important to note that the FCNN layers are the same across time steps i.e. the weights of the connections are same across time steps, where as the weights of the LSTM cells are different across time steps. The Time Distributed Architecture was chosen to mimic the cell structure of the CFAR detector. The dimensions of the neural network layers are given in Table 4.4.

LAYER	SET 1	SET 2
Input Layer	3x1020	3x1400
Time Distributed FCNN Layer 1	3x1020	3x1400
Time Distributed FCNN Layer 2	3X256	3X256
LSTM Layer 1	3x256	3x256
LSTM Layer 2	3x256	3x256
Time Distributed FCNN Layer 3	3x1	3x1

Table 4.4: Dimensions of neural network layers

The activation function used in the first two FCNN layers is ReLU activation and the Sigmoid activation function is used in the final layer.

4.2.2.2 Hyperparameters

The hyperparameters fixed for training the network are given in Table 4.5

HYPERPARAMETER	SET 1	SET 2
Train : Test Data Split	8000:2000	8000:2000
Loss Function	BCE	BCE
Optimizer	Adam	Adam
Learning Rate	10^{-4}	10^{-4}
Learning Rate Decay	10^{-6}	10^{-5}
Batch Size	32	32
Maximum number of Epochs	300	300

Table 4.5: Hyperparameters

The hyperparameters are similar to the ones used for training the FCNN model. It is common for neural networks to overfit when trained for many epochs. A technique to avoid this, is to stop training just as the network starts to overfit. This is known as early stopping. This technique was employed in the training of the model where the validation loss is observed during training and is stopped if the validation loss does not decrease for 25 consecutive epochs. When the training is completed the model with the least validation loss is saved for testing.

4.2.2.3 Results

In this section the performance of the Time Distributed FCNN-LSTM Architecture on signal datasets of the two sets of parameters is presented. The accuracy of the neural network on the test set is used as a measure of it's performance. While the architecture predicts the presence of radar signal in all the three cells, only predictions made by the neural network for the CUT are considered for computing the accuracy. This is because in the signal datasets the radar signal is never present in the adjacent cell, and if the predictions for all the cells are considered then it would lead to high accuracy values despite many wrong predictions. Hence the accuracy of predictions for the CUT alone, would be more meaningful. This also allows for a fair comparison with the baseline algorithm as the CFAR detector detects the presence of radar signal in the CUT only. The accuracy for a single configuration of the SNR and interference power is obtained from training a separate neural network for that model.

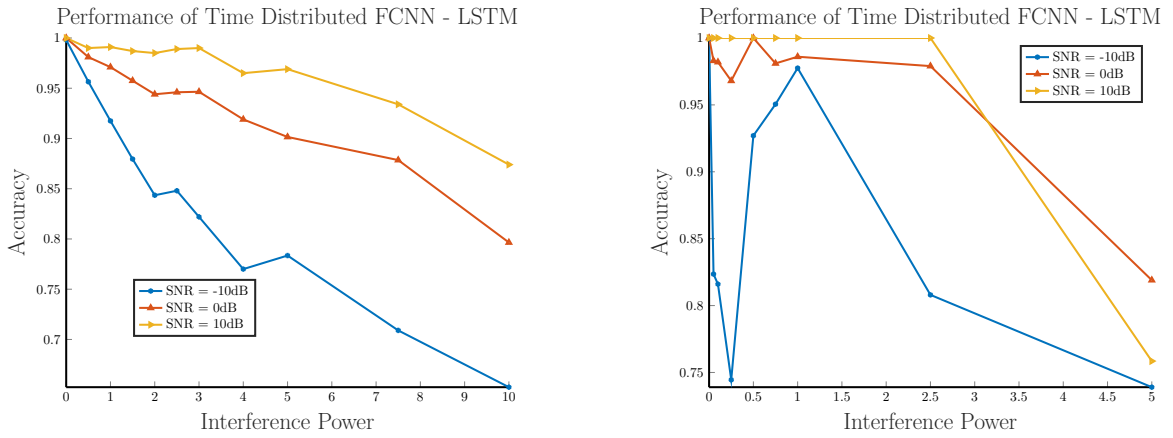

(a) Wide band interference

(b) Narrow band interference

Figure 4.6: Performance of Time Distributed FCNN - LSTM network under wide band and narrow band interference for different SNRs (Set 1)

The Figure 4.6 (a) shows the wideband performance of the Time Distributed FCNN-LSTM architecture for the first set of parameters. From the plot, it can be observed that the performance of the network worsens with the increase in the interference power. It can also be observed that the performance improves significantly with the increase in SNR and the deterioration of performance due to higher interference power is much lesser for higher SNRs. For the narrow band interference case shown in Figure 4.6 (b) , the improvement of performance due to increase in SNR is also evident. On comparing the narrow band and wide band performances of the network it can be observed that despite the in-band (with respect to the radar signal) power being significantly high for the narrow band interference case , the performance is comparable and sometimes even better than that of the wide band interference case. It can also be seen that the accuracy of the architecture for the narrow band case is 100 % when the SNR is 10dB and interference power is less than 3.

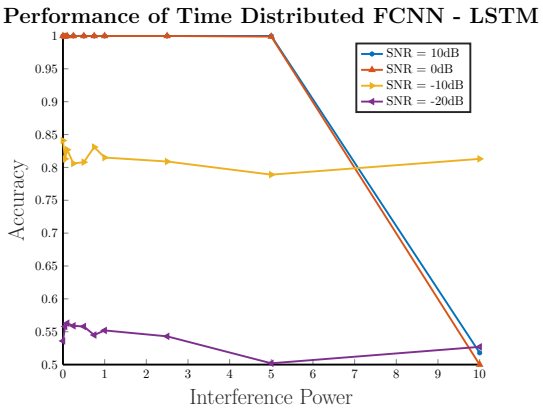

(a) Narrow band interference 1

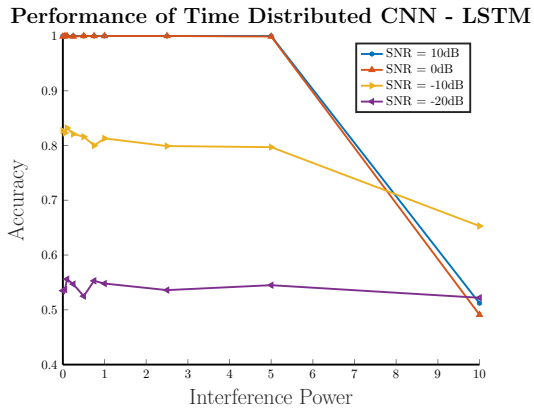

(b) Narrow band interference 2

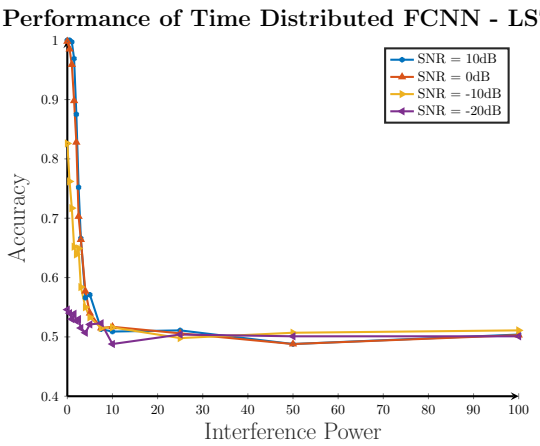

(c) Wide band interference

Figure 4.7: Comparison of performance of Time Distributed FCNN - LSTM network under wide band interference and narrow band interference (Set 2)

The narrow band performance of the Time Distributed FCNN LSTM architecture as shown in the Figures 4.7 (a) and (b) remains almost constant at low interference powers (< 5) and at interference power 10 the performance appears to drastically drop under for high SNRs. For both the interference types, a boost in performance with increase in SNR can be observed for lower interference powers. The wide band performance of the network as shown in Figure 4.7(c) appears to gradually degrade with increase in interference power and the performance improves with the increase in SNR at lower interference powers(<10). At very high interference powers the architecture

performs poorly irrespective of the SNR.

4.2.3 Time Distributed CNN - LSTM

4.2.3.1 Architecture

In this section we present an architecture which uses a combination of Time Distributed 1D CNN layers and LSTM layers. The architecture consists of a Time Distributed 1D CNN layer with 32 filters each of length 1000 followed by three LSTM layers and a final Time Distributed FCNN layer. The architecture is shown in Figure 4.8

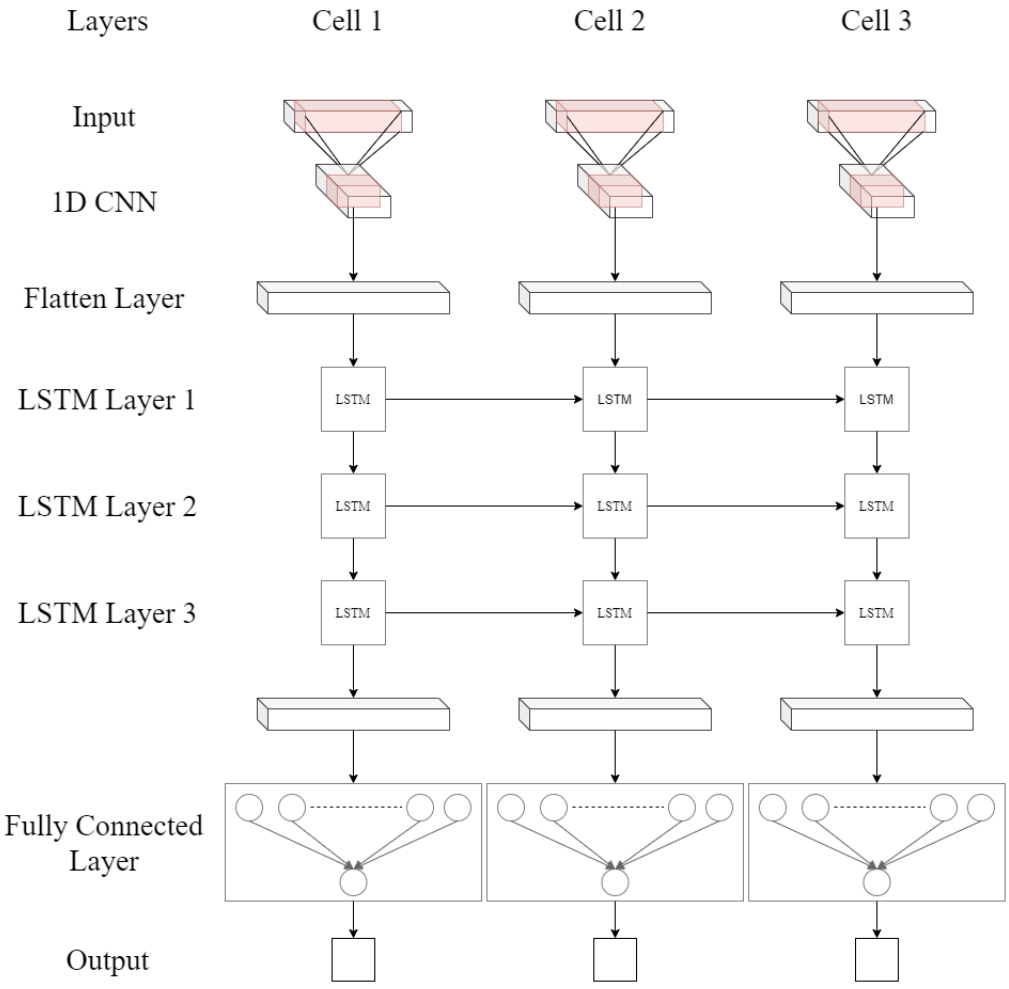

Figure 4.8: Time Distributed CNN - LSTM architecture

The design of this architecture mimics the structure of the CFAR detector. The Time Distributed wrapper allows for a structure similar to the cells of the CFAR detector. The length of the filter for the 1D CNN was chosen to be 1000 to mimic the matched filter which convolves a template of length 1000 (the signal length), but unlike the matched filter which convolves a single template, the convolutional layer convolves 32 such templates to each time step. The resulting 32 filter outputs for each time step are flattened (concatenated) resulting in a single vector for each time step. These vectors are then passed through the three LSTM layers and then through a Time Distributed FCNN layer. The dimensions of the neural network layers are given in Table 4.6.

LAYER	SET 1	SET 2
Input Layer	3x1020	3x1400
CNN Layer Filters	32x1000	8x1000, 8X200, 16X100, 32x50
Time Distributed Flatten Layer	3x672	3x1728
LSTM Layer 1	3x672	3x1728
LSTM Layer 2	3x672	3x1728
Time Distributed FCNN Layer	3x1	3x1

Table 4.6: Dimensions of neural network layers

Significant changes to the architecture are made for the second set of parameters, this is because of the greater signal dimension. If the architecture for the first set was used for the second set , the output from the convolutional layer would be too big to handle. In order to make the output size manageable, multiple convolutional layers were used to reduce the output dimensions. Pooling layers were avoided to prevent major loss of information. The activation function used in the CNN layer is ReLU activation and the Sigmoid activation function is used in the final layer.

4.2.3.2 Hyperparameters

The hyperparameters fixed for training this network are shown in 4.7

HYPERPARAMETER	SET 1	SET 2
Train : Test Data Split	8000:2000	8000:2000
Loss Function	BCE	BCE
Optimizer	Adam	Adam
Learning Rate	10^{-4}	10^{-4}
Learning Rate Decay	10^{-6}	10^{-5}
Batch Size	32	32
Maximum number of Epochs	300	300

Table 4.7: Hyperparameters

The hyperparameters used for training this network are the same as the ones used for training the FCNN-LSTM network. Early stopping technique was employed for training this network too.

4.2.3.3 Results

In this section, the performance of the Time Distributed CNN - LSTM network is discussed. Prediction Accuracy of the test set is considered as the metric for evaluating the performance of the neural network. The performance of the neural network for different SNRs under wide band and narrow band interference is shown in Figures 4.9 (a) and (b) respectively.

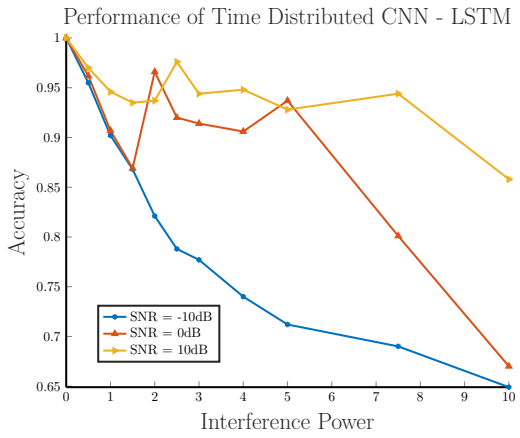

(a) Wide band interference

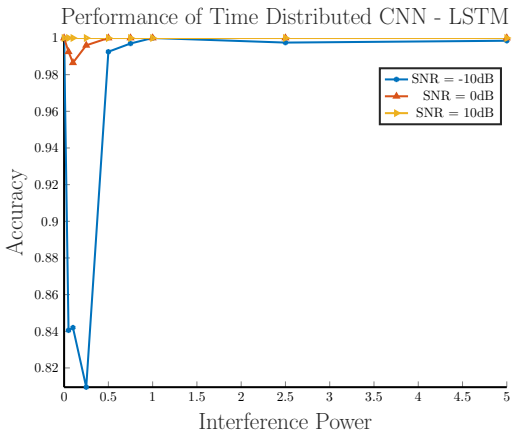

(b) Narrow band interference

Figure 4.9: Performance of Time Distributed CNN - LSTM network under wide band and narrow band interference for different SNRs (Set 1)

Under wide band interference , the performance of the network decreases with increase in interference power and an increase in SNR is able to provide a significant boost to the detection performance. The performance of the architecture under narrow band interference is exceptional with 100% accuracy for almost every configuration of SNR and interference. It can also be observed that performance of the CNN under the narrow band interference exceeds its performance under wide band interference.

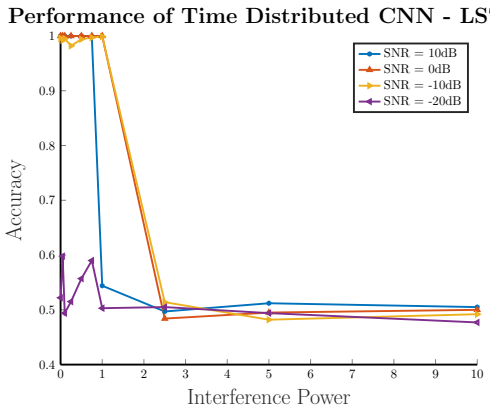

(a) Narrow band interference 1

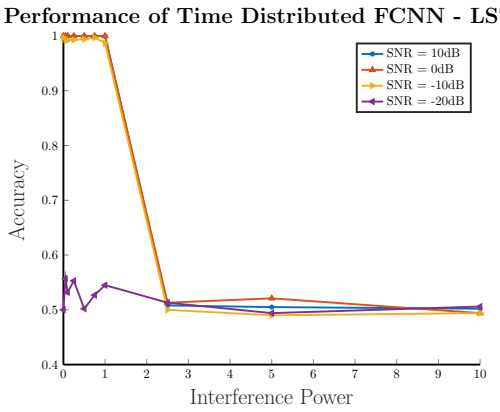

(b) Narrow band interference 2

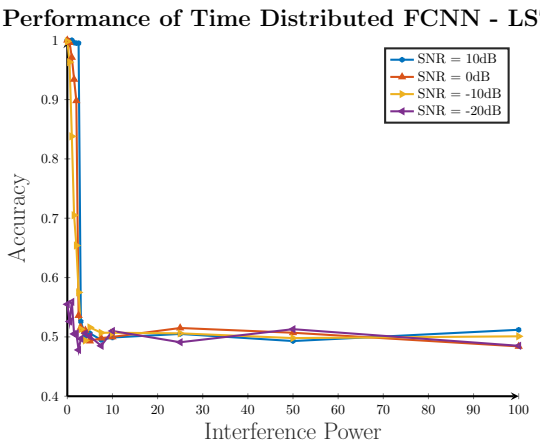

(c) Wide band interference

Figure 4.10: Performance comparison of Time Distributed CNN - LSTM detector under wide band and narrow band interference (Set 2)

The Figures 4.10 (a) and (b) show the narrow band performance of the Time Distributed CNN-LSTM architecture. The detection accuracy is 100% at very low(< 3) interference powers and high SNRs but decreases for interference powers greater than 3. The performance is almost similar under both the narrow band interference. The wide band performance of the network as shown in Figure 4.10 (c) appears to degrade with increase in interference power and performs poorly at interference powers greater than 3. The improvement in performance with the increase in SNR can be observed at very low interference powers(<3).

4.3 Performance Comparison of Neural Network Based Detectors and CFAR Detector

4.3.1 First Set of Parameters

The detection performance of the neural network architectures explored for the first set of parameters have shown similar characteristics. Three main similarities can be observed in their performance. The first observation is that under wide band interference, the performance of all the neural networks deteriorated with the increase in interference power. The next observation is that the narrow band performance of the network was significantly better than the wide band performance. The third observation is that the increase in SNR often resulted in a significant boost in detection performance. These observations are quite in contrary to the performance characteristics of the CFAR detector. While the performance of the CFAR detector also deteriorates with increase in interference power, it's performance under narrow band interference is significantly worse than under wide band interference and an increase in SNR of the signal did not cause any significant improvement to the performance of the CFAR detector.

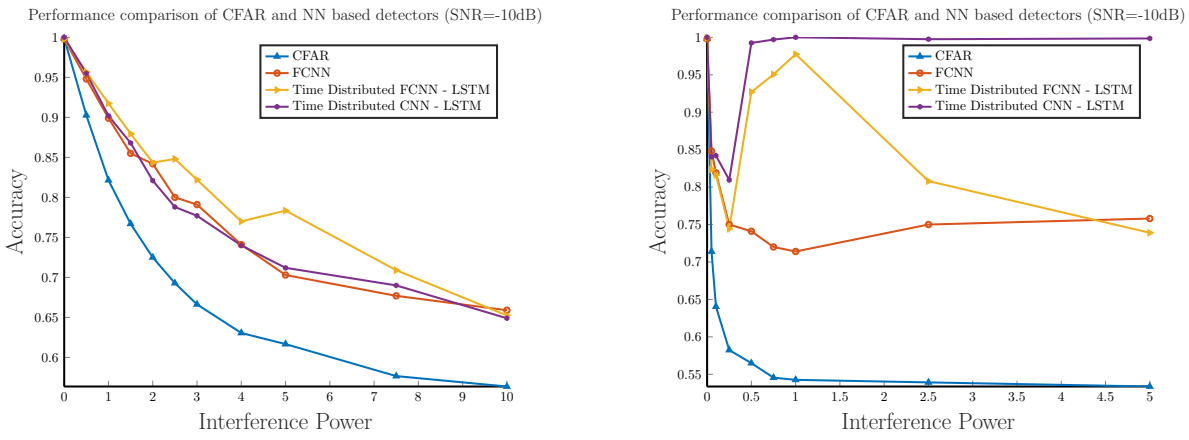

(a) Wide band interference

(b) Narrow band interference

Figure 4.11: Performance comparison of CFAR detector and Neural Network based detectors for SNR = -10dB (Set 1)

From the Figures 4.11 (a) and (b) it can be observed that under wide band interference the

neural networks outperform the CFAR detector by a considerable margin and under narrow band interference they outperform by a significant margin.

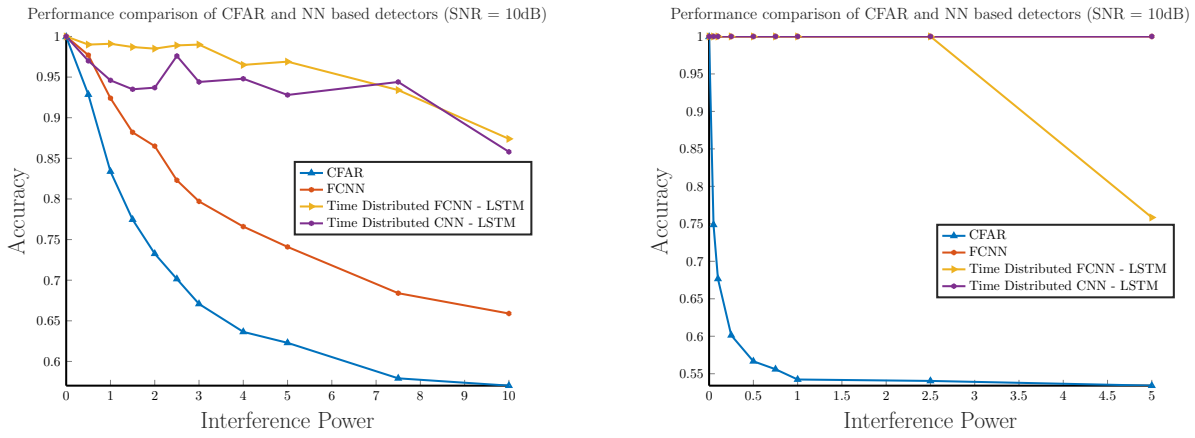

(a) Wide band interference

(b) Narrow band interference

Figure 4.12: Performance comparison of CFAR detector and Neural Network based detectors for SNR = 10dB (Set 1)

The Figures 4.12 (a) and (b) show the performance of Neural networks and CFAR detector at SNR = 10dB. With a further increase in SNR, a similar trend is observed where the performance for the wide band interference case, of Time Distributed FCNN - LSTM and Time Distributed CNN-LSTM networks is seen to improve further, while the performance of FCNN (three cell case) and the CFAR detector do not change significantly. The performance for the narrow band interference case of all neural networks improve to 100% accuracy for most interference powers while the CFAR detector performance remains unchanged. From the performance of all the detectors it can be said that the Time Distributed FCNN-LSTM architecture offers a better performance for the wide band interference case and the Time Distributed CNN-LSTM offers an exceptional performance under narrow band interference.

4.3.2 Second Set of Parameters

The performance comparison of the networks on the signal datasets from the second set of parameters is shown in Figures 4.13, 4.14 and 4.15. It has been observed that all networks perform poorly under SNR = -20dB and at interference powers greater than 10. Thus the SNR range -10dB to 10 dB and interference power range 0 to 10 allow for a more meaningful comparison of the network performance.

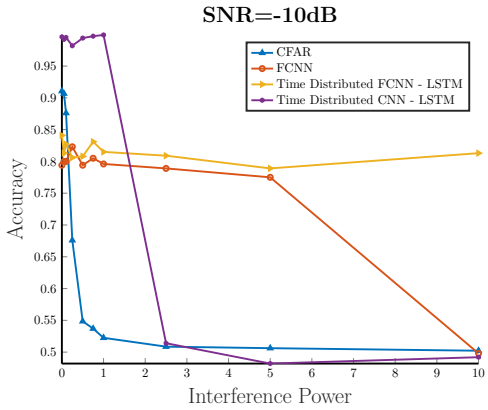

(a) Narrow band interference

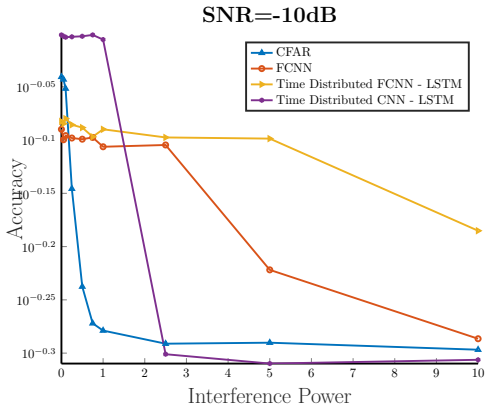

(b) Narrow band interference

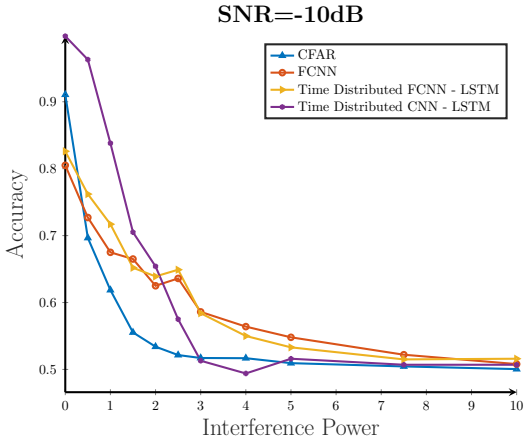

(c) Wide band interference

Figure 4.13: Performance comparison of CFAR detector and Neural Network based detectors for SNR = -10dB (Set 2)

The Figures 4.13 (a) and (b) compare the performance of the detectors for SNR = -10dB. It can be observed that at very low interference powers (< 3) the CNN-LSTM architecture outperforms all the detectors and at higher interference powers the FCNN-LSTM architecture performs the best. Under wide band interference as shown in Figure 4.13 at very low interference powers (< 3) the CNN-LSTM performs the best while at higher powers the three cell FCNN architecture outperforms the rest. It can also be observed that neural network based architectures significantly outperform the CFAR detector under most configurations of SNR and interference powers.

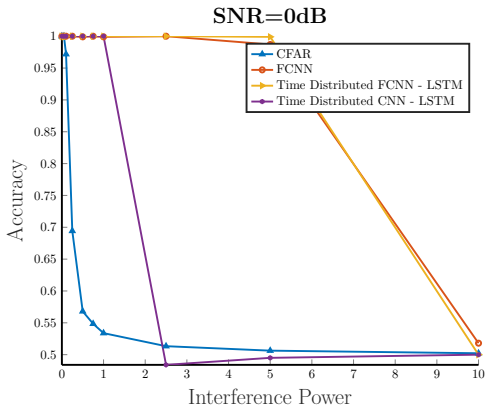

(a) Narrow band interference

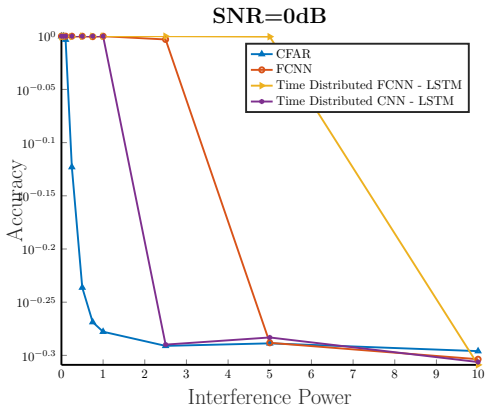

(b) Narrow band interference

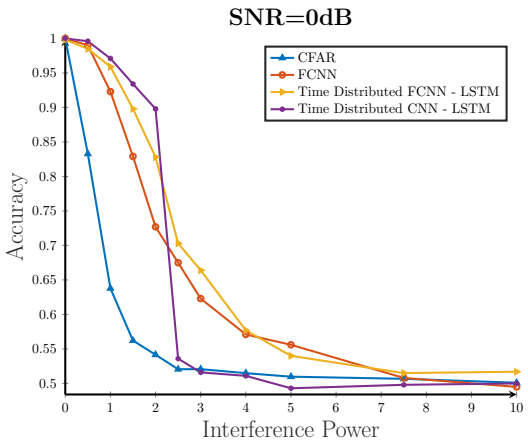

(c) Wide band interference

Figure 4.14: Performance comparison of CFAR detector and Neural Network based detectors for SNR = 0dB (Set 2)

The Figures 4.14 (a), (b) and (c) show the performance of the detectors for SNR = 0dB. With the increase in SNR a boost in performance of all the neural network based detectors can be observed while the performance of the CFAR detector remains about the same. Under narrow band interference the FCNN-LSTM architecture outperforms all the network. For wide band interference it can be observed that at very low interference powers (< 3) the CNN-LSTM architecture outperforms all the detectors and at higher interference powers the FCNN-LSTM architecture performs the best.

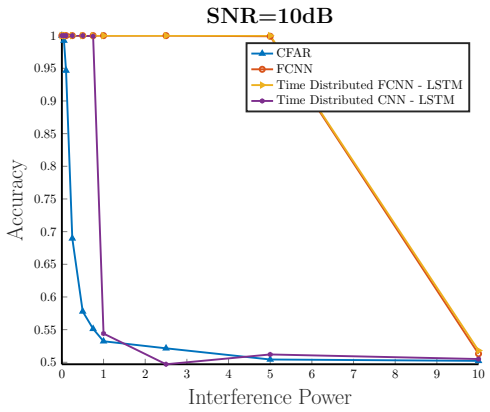

(a) Narrow band interference

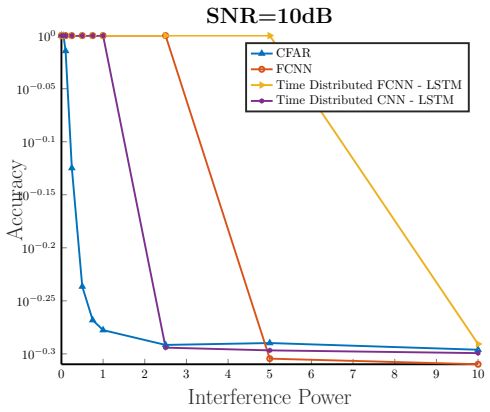

(b) Narrow band interference

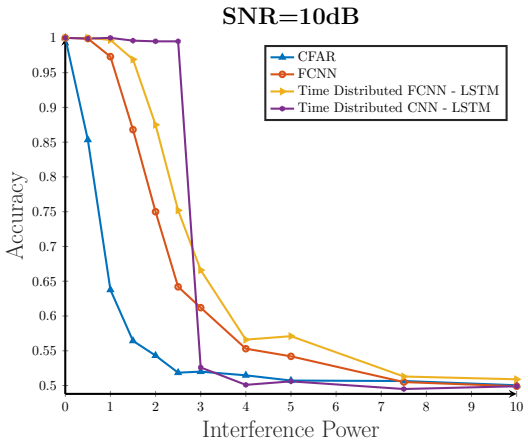

(c) Wide band interference

Figure 4.15: Performance comparison of CFAR detector and Neural Network based detectors for SNR = 10dB (Set 2)

The performance of the detectors for SNR = 10dB can be seen in the Figures 4.15 (a), (b) and (c) . The further increase in SNR appears to boost the performance of all the neural network based detectors under wide band interference especially at low interference powers. Under narrow band interference the FCNN-LSTM architecture outperforms all the detectors. For wide band interference it can be observed that the CNN-LSTM architecture outperforms all the detectors at very low interference powers (< 3), and at higher interference powers the FCNN-LSTM architecture outperforms the rest.

Under both the sets of parameters it can be observed that neural network based detectors significantly outperform the CFAR detector for most configurations of SNR and interference powers. The significant performance improvement of the neural networks show that the neural networks are able to implement some form of filtering better than a traditional matched filter. The neural networks are able to utilize the inherent structure of the interference signal to their advantage. Their exceptional performance under narrow band interference can be attributed to this quality of neural networks. Due to the symbol rate of the interference signal being low (10KHz) in the narrow band case, the number of symbols in a time duration equal to the pulse duration of the radar (0.1 ms) is less (1 symbol), where as in the case of wide band interference where the symbol rate is high (1 MHz) , there would be more symbols(100) for the same duration. The neural network is able to easily estimate the symbols with very high in-band power in the case of narrow band interference. Where as the neural networks find it difficult to estimate many symbols with low in-band power in the case of wide band interference. It is also important to note that the radar signal power is fixed and an increase in SNR is obtained through a decrease in noise variance. So the boost in performance due to the increase in SNR can be explained as the neural networks being able to estimate the interference signal better due to the reduction in noise power. Thus higher in-band interference power and lower noise power can be favourable for neural networks while any in-band interference can significantly reduce the performance of the CFAR detector.

5. CONCLUSION AND FUTURE WORK

5.1 Conclusion

Coexistence of Radar and Communications is an important research area which can contribute towards efficient utilization of the already congested RF spectrum. Enabling Radar systems to function amidst communication interference is a major step in this direction. This thesis proposes a machine learning based approach to detect radar signals corrupted with communication interference and noise. The matched filtering based Constant False Alarm Rate (CFAR) detector was considered as a baseline for evaluating the performance of neural network architectures. Three neural network architectures were designed and evaluated. The first architecture is a Fully Connected Neural Network (FCNN) architecture which consists of two hidden layers and an output layer. The second architecture is called as Time Distributed FCNN - LSTM architecture which is made of two Time Distributed FCNN layers combined with two LSTM layers and a final Time Distributed FCNN layer as the output layer. The third architecture is called as Time Distributed CNN - LSTM architecture which consists of a single 1D CNN layer combined with three LSTM and a final Time Distributed FCNN layer as the output layer. The performance of these detectors were evaluated for two sets of parameters each with two types of interference signals which are narrow band interference and wide band interference.

The simulation results of the baseline CFAR detector showed that an increase in interference power resulted in deterioration of detection performance and an increase in SNR (from -10 dB to 10dB) did not cause any significant improvement in detection performance. It was also observed that the performance of the CFAR detector was much worse for the narrow band interference case than for the wide band case, which can be attributed to the fact that the narrow band interference had higher in-band power than the wide band interference.

The simulation results of the neural network architecture showed that most of the architectures outperformed the CFAR detector in most configurations of SNR and interference power by a sig-

nificant margin. This shows that the neural network architectures are able to learn some form of filtering better than the matched filter. The performance of all the neural networks had a few traits in common. The first observation is that an increase in interference power resulted in deterioration of performance of the neural networks under the wide band interference case. The second observation is that an increase in SNR (from -10dB to 10dB) resulted in a significant increase in the performance of the Neural Networks which was unlike that in CFAR detector. The last observation was that all the neural networks performed significantly better under narrow band interference than under wide band interference. This was opposite to the performance of CFAR detector which did worse under narrow band interference.

This improved performance of neural networks under narrow band interference can be attributed to the fact that narrow band interference has low symbol rate and high in-band power which makes it easy for a neural network to estimate the interference and cancel it out, while the high symbol rate and low in-band power of wide band interference makes it difficult. The boost in performance due to increased SNR can be explained as the reduction of noise power making it easier for neural networks to estimate the interference. These results show the potential of neural network based detectors for the problem of radar detection under communication interference.

5.2 Future Work

The significant performance improvement of neural network architectures over the CFAR detector opens up a lot of possibilities for future work. A few of them are listed below.

- The diversity of neural network architectures always leaves a possibility for a better performing neural network. Hence better architectures and training techniques could be explored for the same problem.

- Theoretical limits on radar signal detection under communication interference can be studied as this will aid in determining when to stop the search for a better neural network.

- For this research work separate neural network models were trained for different configurations of SNR and Interference power. Neural Network architectures can be designed and

trained to perform under any SNR or Interference power resulting in a more robust detector.

- The performance of neural networks can also be evaluated for different fading models and propagation loss models.
- The filtering being performed by neural networks can be extracted and possibly interpreted to gain better theoretical understanding of filter designs for such detection scenarios.

REFERENCES

[1] "Cisco annual internet report (2018–2023) white paper." [Online] Available: https://www.cisco.com/c/en/us/solutions/collateral/executive-perspectives/annual-internet-report/white-paper-c11-741490.html , Accessed: 15 June 2020.

[2] B. Paul, A. R. Chiriyath, and D. W. Bliss, "Survey of RF communications and sensing convergence research," *IEEE Access*, vol. 5, pp. 252–270, 2017.

[3] L. Zheng, M. Lops, Y. C. Eldar, and X. Wang, "Radar and communication coexistence: An overview: A review of recent methods," *IEEE Signal Processing Magazine*, vol. 36, pp. 85–99, Sep 2019.

[4] D. P. Zilz and M. R. Bell, "Statistical modeling of wireless communications interference and its effects on adaptive-threshold radar detection," *IEEE Transactions on Aerospace and Electronic Systems*, vol. 54, pp. 890–911, Apr 2018.

[5] A. Dimas, B. Li, M. Clark, K. Psounis, and A. Petropulu, "Spectrum sharing between radar and communication systems: Can the privacy of the radar be preserved?," in *2017 51st Asilomar Conference on Signals, Systems, and Computers*, IEEE, Oct 2017.

[6] N. Nartasilpa, D. Tuninetti, N. Devroye, and D. Erricolo, "Let's share CommRad: Effect of radar interference on an uncoded data communication system," in *2016 IEEE Radar Conference (RadarConf)*, IEEE, May 2016.

[7] N. Nartasilpa, A. Salim, D. Tuninetti, and N. Devroye, "Communications system performance and design in the presence of radar interference," *IEEE Transactions on Communications*, vol. 66, pp. 4170–4185, Sep 2018.

[8] J. Qian, M. Lops, L. Zheng, X. Wang, and Z. He, "Joint system design for coexistence of MIMO radar and MIMO communication," *IEEE Transactions on Signal Processing*, vol. 66, pp. 3504–3519, Jul 2018.

[9] J. A. Mahal, A. Khawar, A. Abdelhadi, and T. C. Clancy, "Spectral coexistence of MIMO radar and MIMO cellular system," *IEEE Transactions on Aerospace and Electronic Systems*, vol. 53, pp. 655–668, Apr 2017.

[10] D. Cohen, K. V. Mishra, and Y. C. Eldar, "Spectrum sharing radar: Coexistence via xampling," *IEEE Transactions on Aerospace and Electronic Systems*, vol. 54, pp. 1279–1296, Jun 2018.

[11] J. R. Guerci and R. M. Guerci, "Rast: Radar as a subscriber technology for wireless spectrum cohabitation," in *2014 IEEE Radar Conference*, IEEE, May 2014.

[12] B. Li and A. P. Petropulu, "Joint transmit designs for coexistence of MIMO wireless communications and sparse sensing radars in clutter," *IEEE Transactions on Aerospace and Electronic Systems*, vol. 53, pp. 2846–2864, Dec 2017.

[13] A. Aubry, A. D. Maio, M. Piezzo, and A. Farina, "Radar waveform design in a spectrally crowded environment via nonconvex quadratic optimization," *IEEE Transactions on Aerospace and Electronic Systems*, vol. 50, pp. 1138–1152, Apr 2014.

[14] A. Aubry, A. D. Maio, Y. Huang, M. Piezzo, and A. Farina, "A new radar waveform design algorithm with improved feasibility for spectral coexistence," *IEEE Transactions on Aerospace and Electronic Systems*, vol. 51, pp. 1029–1038, Apr 2015.

[15] S. Sodagari, A. Khawar, T. C. Clancy, and R. McGwier, "A projection based approach for radar and telecommunication systems coexistence," in *2012 IEEE Global Communications Conference (GLOBECOM)*, IEEE, Dec 2012.

[16] H. Deng and B. Himed, "Interference mitigation processing for spectrum-sharing between radar and wireless communications systems," *IEEE Transactions on Aerospace and Electronic Systems*, vol. 49, pp. 1911–1919, Jul 2013.

[17] F. Liu, C. Masouros, A. Li, T. Ratnarajah, and J. Zhou, "MIMO radar and cellular coexistence: A power-efficient approach enabled by interference exploitation," *IEEE Transactions on Signal Processing*, vol. 66, pp. 3681–3695, Jul 2018.

[18] N. Nartasilpa, S. Shahi, A. Salim, D. Tuninetti, N. Devroye, D. Erricolo, D. P. Zilz, and M. R. Bell, "Let's share CommRad: Co-existing communications and radar systems," in *2018 IEEE Radar Conference (RadarConf18)*, IEEE, Apr 2018.

[19] M. I. Skolnik, *Introduction to Radar Systems*. New York: McGraw-Hill, 3rd edition ed., 2001.

[20] J. R. Klauder, A. C. Price, S. Darlington, and W. J. Albersheim, "The theory and design of chirp radars," *The Bell System Technical Journal*, vol. 39, no. 4, pp. 745–808, 1960.

[21] B. R. Foy, J. Theiler, and A. M. Fraser, "Decision boundaries in two dimensions for target detection in hyperspectral imagery," *Optics Express*, vol. 17, p. 17391, Sep 2009.

[22] Z. Qin, H. Ye, G. Y. Li, and B.-H. F. Juang, "Deep learning in physical layer communications," *IEEE Wireless Communications*, vol. 26, pp. 93–99, Apr 2019.

[23] F. A. Aoudia and J. Hoydis, "End-to-end learning of communications systems without a channel model," in *2018 52nd Asilomar Conference on Signals, Systems, and Computers*, pp. 298–303, 2018.

[24] D. George and E. Huerta, "Deep neural networks to enable real-time multimessenger astrophysics," *Physical Review D*, vol. 97, Feb 2018.

[25] S. Hochreiter and J. Schmidhuber, "Long short-term memory," *Neural Computation*, vol. 9, pp. 1735–1780, Nov 1997.

[26] D. Kingma and J. Ba, "Adam: A method for stochastic optimization," *International Conference on Learning Representations*, Dec 2014.